



@2012

AgnieszkaKlimczak

ALL RIGHTS RESERVED

Host-Guest Complexes
Their Characterization by Spectroscopic Tools
and Photoinduced Electron Transfer on Metal Oxide Surfaces

by

AGNIESZKA KLIMCZAK

A Dissertation submitted to the

Graduate School-Newark

Rutgers, The State University of New Jersey

In partial fulfillment of the requirements

For the degree of

Master of Science

Graduate Program in Department of Chemistry

Written under the direction of

Professor Elena Galoppini

And approved by

Newark, New Jersey

October, 2012

Abstract
Host-Guest Complexes
Their Characterization by Spectroscopic Tools
and Photoinduced Electron Transfer on Metal Oxide Surfaces
BY
AGNIESZKA KLIMCZAK

Dissertation Director:
Professor Elena Galoppini

This thesis describes the host-guest chemistry between two different kind of hosts such as Octa Acid (OA) and cucurbit[7]uril (CB[7]), with various guests.

First, we demonstrated that encapsulation of a guest, Coumarin 153 (C-153), within the macrocyclic host cavity (OA as a host) can be used as alternative method for binding the host-guest capsule onto semiconductor surfaces (MO_n functionalization) by using the $-\text{COOH}$ anchoring groups of OA. The complex (abbreviated as C-153@OA_2) is used to exhibit photoinduced electron transfer process of the donor and the acceptor, which plays an important role in commercial applications such as Dye-sensitized solar cells (DSSCs). These novel hybrid systems overcome problems such as aggregation and photodegradation of organic dyes upon exposure to light. By shielding the guests from the heterogeneous interfaces, the dyes' photophysical and electrochemical properties are different than those obtained by modification with anchoring groups for direct attachment

to semiconductor surfaces. The examination of the C-153@OA₂ capsule for the electron transfer to TiO₂ has shown that it requires conditions which are dependent on the complex stability (pH=7). Despite the fact, that OA is more soluble in basic conditions, the injection process from the C-153@OA₂ capsule to TiO₂ surface happens under neutral conditions (pH=7). In addition, the pH dependence on the emission spectra of C-153@OA₂ in water were recorded and we conclude that the capsule is most stable at pH=7. Also, the emission spectra of C-153@OA₂ on TiO₂ films (λ_{ex} =420 nm; pH=7) was quenched; however, in a case of functionalized ZrO₂ films, which were used for control experiments, the emission spectrum shows λ_{max} ~ 500 nm (similar as that for solution spectra) that gives proof of the photoinduced electron transfer between C-153@OA₂ capsule and MO_n surface. Moreover, FT-IR-ATR spectra of TiO₂ and ZrO₂ functionalized films (with C-153@OA₂; pH=7) confirmed the binding of the complex onto the MO_n surfaces.

Second, Raman spectroscopy was used as a novel method for structural characterization and the proof of binding of the host-guest complex of ferrocene@cucurbit[7]uril (Fc@CB[7]). The UV-Vis spectra of the Fc@CB[7] complex were monitored as a function of pH (pH<2 and 7) and the time of complex formation in de-aerated conditions. From those spectra, the formation of the Fc@CB[7] complex was found to form at pH=7 after one and a half weeks at λ_{max} ~402 nm; however, at pH<2 the complex formation was faster; but because of the acidic conditions, the guest was oxidized to ferroceniumion (Fc⁺), and both the neutral and the positively-charged (oxidized) form of ferrocene complexes were observed at λ_{max} ~625 nm and ~440 nm. MALDI-FTMS was used for detection of the complex formed; this confirmed that the

Fc@CB[7] 1:1 complex exists under these experimental conditions. Infrared spectroscopy is not suitable to study low frequency vibrations ($<600\text{ cm}^{-1}$) and the IR bands of CB[7] overlap with those deriving from the encapsulated guest, so it is difficult to distinguish the spectra of the complex. Therefore, Raman spectroscopy was used to observe shifts of specific vibrational modes between the spectra of the complex and that of unbound guest and host. The shifts of specific vibrational modes (or the lack thereof) deriving from different parts of the Fc@CB[7] complex, were easily observed by Raman spectroscopy and gave evidence of Fc guest encapsulation within the CB[7] macrocyclic host in the solid state. In addition, Raman spectroscopy permits for some insight at the molecular level, of the structural and electronic interactions that coexist upon formation of the complex, such as low frequency bands of Fc, the symmetric Fe-Cp ring stretch at 309 and 391 cm^{-1} , which shift to 318 and 400 cm^{-1} . Also, other vibrational modes were localized on CB7 host (weak interactions between Cp rings and the CB7 interior), which exist upon inclusion of Fc in the CB7 cavity, such as CB ring distortion modes at 442 and 833 cm^{-1} that involve deformation of the host cavity interior upon encapsulation of Fc.

Acknowledgement

I would like to express my sincere thanks to my supervisor, Professor Elena Galoppini, for her kindness, help, long-term support and guidance she has given me during my studies. Especially, I am thankful for her advice and patience during correcting my thesis. It has been a pleasure studying in and being a member of her research group.

I am also grateful to my committee members, Prof. Jenny Lockard and Prof. Roger Lalancette of Rutgers University, Newark, for their help and time in reading and correcting my thesis.

My gratitude also goes to all members of the Galoppini group, both past and present, Dr. Alfred Lee, Dr. Yongyi Zhang, Dr. Marina Freitag, Andrew Kopecky, KeyurChitre, and Yan Cao, for all of their assistance and teaching me all the techniques required in our lab, and for their support and motivation.

I greatly appreciate the faculty members of the Chemistry Department, especially Prof. PiotrPiotrowiak and Prof. Rudolph Kluiber, for accepting me as a teaching assistant, their knowledge, research advice, excellent teaching and guiding me throughout my education endeavors.

I would like to take this opportunity to thanks the members of the chemistry office, Judy Slocum, Monika Dabrowski, Lorraine McClendon, and also the staff of both the Department of Chemistry and Rutgers University for their helpfulness.

Finally, I am also grateful for my husband and children for their love, encouragement and patience during my studies.

Table of Contents

ABSTRACT.....	ii
ACKNOWLEDGEMENT.....	v
LIST OF TABLES.....	viii
LIST OF FIGURES.....	ix
<u>CHAPTER ONE</u>	1
<u>SUPRAMOLECULAR CHEMISTRY-HOST-GUEST COMPLEXES, THEIR INTERACTIONS WITH NANOSTRUCTURED METAL OXIDE SURFACES, AND THEIR RECOGNITION BY SPECTROSCOPIC TOOLS</u>	1
INTRODUCTION.....	2
1.1 Supramolecular Chemistry.....	2
1.2 The "Host-Guest" Chemistry.....	3
1.3 Supramolecular hosts and their characteristics.....	4
1.3.1 Cucurbiturils.....	6
1.4 Cucurbit[7]uril as a host, its characteristic and application.....	10
1.5 Spectroscopic methods as tools used to identify and characterize H-G complex properties.....	14
1.6 Properties of metal oxide nanoparticles (TiO ₂ , ZrO ₂).....	18
1.6.1 Binding H-G complexes to the Metal Oxide surfaces.....	21
REFERENCES.....	27
<u>CHAPTER TWO</u>	31
<u>MODIFICATION OF TiO₂ SURFACE BY ATTACHMENT OF HEMICARCEPLEX (THE C-153@OA₂ COMPLEX): PHOTOINDUCED ELECTRON TRANSFER BETWEEN C-153 AND TiO₂</u>	31
INTRODUCTION.....	32
EXPERIMENTAL SECTION.....	38
2.1 General.....	38
2.1.1 pH adjustment.....	38
2.1.2 TiO ₂ and ZrO ₂ synthesis.....	39
2.1.3 TiO ₂ /ZrO ₂ films preparation and binding of the C-153@OA ₂ complex to the films.....	42
2.2 Results and Discussion.....	42
2.3 Conclusions.....	47

REFERENCES.....	49
<u>CHAPTER THREE.....</u>	<u>51</u>
<u>RAMAN SPECRTOSCOPY AS A NOVEL PROMISING TOOL FOR ANALYZING A</u>	<u></u>
<u>H-G COMPLEX OF FERROCENE@CB[7].....</u>	<u>51</u>
INTRODUCTION.....	52
EXPERIMENTAL SECTION.....	54
3.1 General.....	54
3.1.1 Synthesis.....	55
3.1.1.1 Cucurbit[7]uril.....	55
3.1.2 Formation of the Fc@CB[7] complex.....	58
3.2 Results and Discussion.....	59
3.3 Conclusion.....	68
REFERENCES.....	70
Curriculum Vitae.....	72

List of Tables

Table 1.1 <i>Parameters of cucurbit[n]urils family.¹¹</i>	7
Table 1.2 <i>Performance of DSSCs prepared from JK-2 as a dye.⁵⁴</i>	25
Table 3.1 <i>Comparison of Raman frequencies of Fc, CB7 and Fc@CB7 and corresponding vibrational mode assignments^a</i>	66

List of Figures

Figure 1.1 Schematic representation of the relationship between molecular and supramolecular chemistry. ³	2
Figure 1.2 X-ray crystal structure of CB[7] (a) and CB[8] (b) complexes. ⁴	3
Figure 1.3 The illustrated examples of some macromolecule hosts. ⁶	5
Figure 1.4 Non X-ray structure of the cucurbit[n]uril family. ¹¹	7
Figure 1.5 The inner and external binding regions behavior (a), and the electrostatic potential surfaces of CB[7] (b). ^{7,11}	8
Figure 1.6 Pathways for CB[n] synthesis. ^{7,11}	9
Figure 1.7 X-ray crystal structure of oxaliplatin/CB[7] complex. ¹¹	10
Figure 1.8 Coordination of sodium ion to the portals of CB[7]. ⁷	12
Figure 1.9 Energy-minimized structures of (a) trans-DAS and (b) cis-DAS inside CB[7] cavity. ¹¹	12
Figure 1.10 Schematic view of the use of CB[7] as a sensor for enzyme assays. ³⁸	14
Figure 1.11 (a) ¹ H-NMR titration plot corresponding for fast exchange equilibration on the NMR time scale; and (b) Schematic NMR spectra of the guest fast and slow exchange equilibria. ⁵	16
Figure 1.12 The UV-Vis Job's plot curve for the 1:1 host-guest complex. ^{3,5}	17
Figure 1.13 Differences in the band gaps	18
Figure 1.14 (a) ATM image of TiO ₂ film and (b) SEM image of ZrO ₂ film. ^{44, 60}	19
Figure 1.15 The mechanism of charge separation in TiO ₂ nanoparticle. ⁷	20
Figure 1.16 Direct binding of the dye molecule (a) on the (MO _n) surfaces and binding through encapsulation inside a host (b). ⁴⁵	21
Figure 1.17 (a) Charge transfer in the azulene@hemispherical complex bound to TiO ₂ , (b) comparison with free, directly-bound dye. ⁴⁹⁻⁵⁰	23
Figure 1.18 (a) Suggested structure of azobenzene dye (I@ α-CD) complex and (b) directly bound azobenzene (2) dye (b) to TiO ₂ . ⁵²	24
Figure 1.19 Proposed attachment of JK-2@β-CD complex to TiO ₂ surface. ⁵⁷	25
Figure 2.1 Structures of Host and Guest Molecules. ⁷	33

Figure 2.2 ^1H -NMR spectra of (i) C-153 in CD_3CN ; (ii)-(iv) C-153 in presence of OA at various guest: host ratios (by fixing host concentration and increasing guest concentration stepwise) (ii) C-153@OA (1:8) $[\text{C-153}] = 0.125 \text{ mM}$ (iii) C-153@OA (1:4) $[\text{C-153}] = 0.25 \text{ mM}$ (iv) C-153@OA (1:2) $[\text{C-153}] = 0.5 \text{ mM}$ (v) 1 mM OA in 10 mM buffered D_2O alone. A-J represents un-complex OA proton signals; a, a'-j represent complexed OA proton signals, and * represents the guest proton signals.²⁴34

Figure 2.3 ^1H -NMR spectra of (i) C-480 in CD_3CN ; (ii)-(iv) C-480 in presence of OA at various guest: host ratios (by fixing host concentration and increasing guest concentration stepwise) (ii) C-480@OA (1:8) $[\text{C-480}] = 0.125 \text{ mM}$ (iii) C-480@OA (1:4) $[\text{C-480}] = 0.25 \text{ mM}$ (iv) C-480@OA (1:2) $[\text{C-480}] = 0.5 \text{ mM}$ (v) 1 mM OA in 10 mM buffered D_2O alone. A-J represents un-complexed OA proton signals; a, a'-j represent complexed OA proton signals, and * represents the guest proton signals.²⁴35

Figure 2.4 DOSY NMR spectra of (a) C-1@OA₂(1:2); (b) C-480@OA₂(1:2) and (c) C-153@OA₂(1:2) complexes. $[\text{OA}] = 1 \text{ mM}$ in 10 mM buffer D_2O and $[\text{C-1}; \text{C-480}; \text{C-153}] = 0.5 \text{ mM}$.²⁴37

Figure 2.5 The experimental set-up for the synthesis of $\text{TiO}_2/\text{ZrO}_2$.²⁹40

Figure 2.6 The picture of the titanium autoclave for $\text{TiO}_2/\text{ZrO}_2$ nanoparticle colloids processes.²41

Figure 2.7 Fluorescence spectra of (a) C-153@OA₂ and (b) C-153 at different pH; $\lambda_{\text{ex}} = 420 \text{ nm}$; $[\text{C-153}] = 1.5 \times 10^{-5} \text{ M}$, $[\text{OA}] = 1 \times 10^{-4} \text{ M}$ in 10 mM sodium tetraborate buffer (from Porel M.).⁷43

Figure 2.8 Fluorescence spectra of (a) C153@OA₂ on TiO_2 and ZrO_2 film, $\lambda_{\text{ex}} = 420 \text{ nm}$; (b) titration of C153@OA₂ with TiO_2 solution; $\lambda_{\text{ex}} = 440 \text{ nm}$; $[\text{C153}] = 1.5 \times 10^{-5} \text{ M}$, $[\text{OA}] = 1 \times 10^{-4} \text{ M}$ in water.⁷45

Figure 2.9 Fluorescence titration spectra of C153@OA₂ with ZrO_2 colloidal solution; $\lambda_{\text{ex}} = 440 \text{ nm}$; $[\text{C153}] = 1.5 \times 10^{-5} \text{ M}$, $[\text{OA}] = 1 \times 10^{-4} \text{ M}$ in water (from Porel M.).⁷45

Figure 2.10 FT-IR-ATR spectra of OA (solid) (I); and of C-153@OA₂ on (a) TiO_2 and (b) ZrO_2 (II).⁷46

Figure 3.1 The schematic illustration of the Fc@CB[7] 1:1 complex.....53

Figure 3.2 ^1H -NMR spectrum of CB[7] in D_2O (3.5-6.4 ppm region).....56

Figure 3.3 Synthesis and separation of CB7.....57

Figure 3.4 Solution UV-Vis spectra of Fc and the Fc@CB7 complex in aerated conditions.....59

Figure 3.5 UV-Vis spectra of the Fc@CB7 complexes (pH<2 and pH=7) de-aerated by freeze-pump-thaw.....	60
Figure 3.6 UV-Vis spectra of Fc@CB7 complexes (pH<2 and pH=7) after 1 ½ weeks.....	60
Figure 3.7 RMS-MALDI full window spectra of Fc@cB7 complex	61
Figure 3.8 HRMS-MALDI calculated isotopic pattern of the Fc@CB7 complex.....	62
Figure 3.9 HRMS-MALDI calculated isotopic pattern of CB7 from the Fc@CB7 complex spectra.....	63
Figure 3.10 FT-IR-ATR spectra of solid CB7 (top), Fc (bottom) and Fc@CB7 with KNO ₃ (middle).....	64
Figure 3.11 (a) Raman spectra of solid ferrocene (red), CB[7] (black) and Fc@CB[7] (blue) with KNO ₃ . Raman spectral ranges of (b) Fc and (c) CB[7] vibrational modes (NO ₃ internal standard peaks indicated with*).....	65

Chapter One

Supramolecular Chemistry – Host-Guest Complexes, Their Interactions With Nanostructured Metal Oxide Surfaces, and Their Recognition by Spectroscopic Tools

Introduction:

1.1 Supramolecular chemistry.

Supramolecular chemistry, which was defined as “chemistry beyond the molecule”² by Jean-Marie Lehn (Nobel Prize Winner in Chemistry) in 1987, is a field of science which studies chemical, physical and biological features of the self-assembled system.

In supramolecular chemistry the molecular components are held together by non-covalent bonds, which are interactions of forces much weaker than classical covalent bonds (this relationship is shown in *Figure 1.1*). These weak interactions include, for instance, hydrogen bonding, van der Waals forces, electrostatic forces and hydrophobic effects.

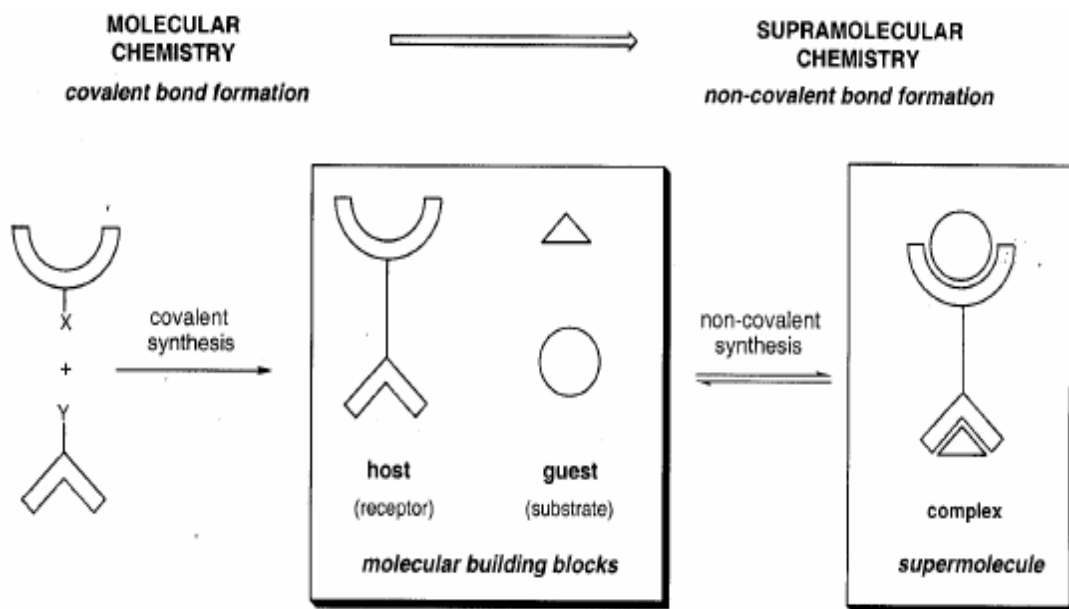


Figure 1.1 Schematic representation of the relationship between molecular and supramolecular chemistry.³

1.2 The “Host-Guest” Chemistry.

Host-Guest (H-G) chemistry is a field of supramolecular chemistry where the host (H) is encapsulated or binds with molecules or ions as guests (G) making a Host-Guest complex (Figure 1.2). This complex between the host and guest molecule is formed by non-covalent forces (hydrogen bonding, hydrophobic interaction, metal-to-ligand binding, etc.). Usually, the host is a synthetic or natural macromolecule with an internal cavity, which serves as a container.⁴ The H-G complex can be non-specific or specific depending on the nature of the two species.⁵

The key aspect of supramolecular H-G chemistry is to generate the set of conditions which will stabilize a H-G complex, such as a suitable solvent, temperature, pH, etc. Some changes in these conditions can decrease the stability of the complex, and lead to its decomplexation.

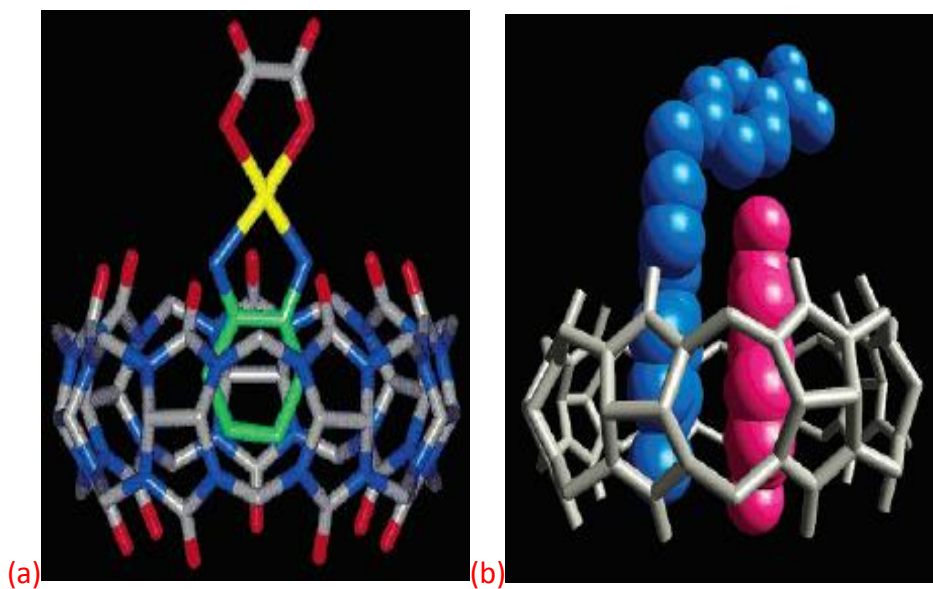


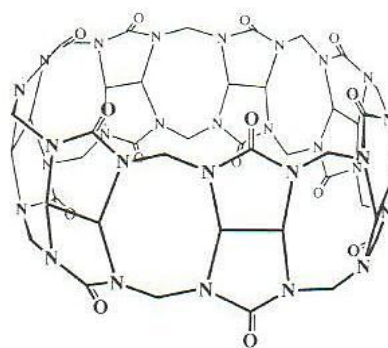
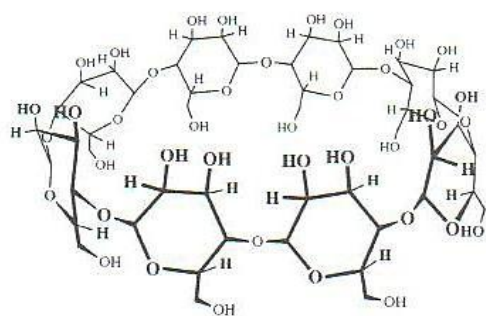
Figure 1.2 X-ray crystal structure of CB[7] (a) and CB[8] (b) complexes.⁴

A *clathrand* is a host, which possesses an extramolecular cavity, with a gap that is made by two or more host molecules bound together. A *cavitand* is a macromolecular host which possesses an intramolecular cavity, so that the interior of the host is available for encapsulation of the guest by binding of the host. Examples of cavitand hosts include: cyclodextrines, cucurbiturils and crown ethers.⁵ Since cavitand structures are often rigid, they are able to form H-G complexes which possess good stability and selectivity with specific electronic properties.

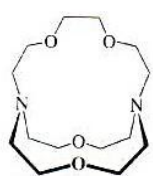
1.3 Supramolecular hosts and their characteristics.

In Host-Guest chemistry supramolecular organic cages are often used as host molecules. Macrocyclic hosts (molecular receptors, which are arranged as a ring) possess multiple binding sites which are able to pre-organize for interaction (binding) with the guest by non-covalent forces. Because of host rearrangement, which is necessary for binding different sizes of guest molecules, the rigid pre-organized host has less freedom and forms a more stable complex leading to increased thermodynamic stability of the complex. Also, the rigidity of macrocyclic hosts allows binding a guest with smaller relative loss of entropy upon its encapsulation.⁶

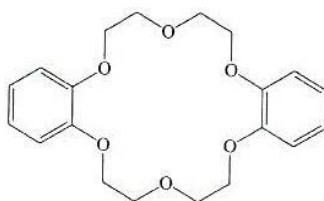
Host organic molecules that are well-known in supramolecular chemistry include: cyclodextrins, calixarenes, crown ethers, cucurbiturils, hemicarceplexes, and carcerands (Figure 1.3). Inorganic networks, such as zeolites (a microporous aluminosilicate mineral) are also capable of encapsulating small organic molecules.⁵



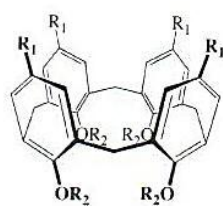
cyclodextrin cucurbituril



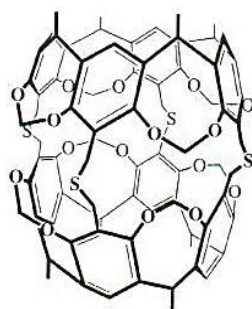
cryptand



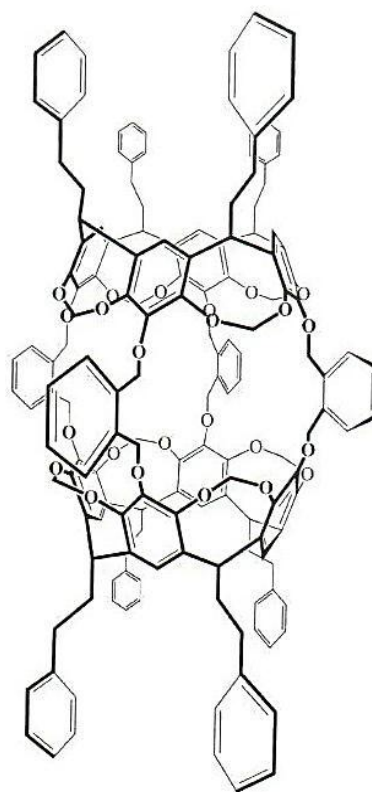
crown ether



calixarene



carcerand



hemicarcerand

Figure 1.3 Examples of some macromolecule hosts.⁶

1.3.1 Cucurbiturils

The focus of this thesis is cucurbiturils. Cucurbit[n]urils (CB[n]) are a family of cyclic oligomers,⁷ where n is the number of repeating glycoluril units which are bridged by twelve methylene groups resembling a pumpkin shape.⁹⁻¹⁰ Therefore, the proposed name cucurbituril was given from the Latin name for pumpkins (“*Cucurbitaceae*”).^{5,9} CBs are formed by the acid-catalyzed condensation of glycoluril with formaldehyde. The synthesis of CB[6] was published in 1905 by Behrend *et al.*;⁸ however, it was initially thought of as across-linked polymer, so it became known as Behrend’s polymer. The structure of this cyclic oligomer was not determined until 1981, when Mock and co-workers characterized the remarkable structure of CB[6] by X-ray crystallography.⁹ During the following years the CB[n] family attracted the interest of many research groups, which focused on developing new synthetic methods for successful preparation other CB[n] homologues. In 1992 Kim, Day, and co-workers independently discovered new separation methods for additional homologues, such as: CB[5], CB[7], CB[8] and CB[10], from the condensation reaction mixture (Figure 1.4).¹²⁻¹⁶ The isolation of CB[n] homologues makes available a family of hosts for different sizes of guests. However, poor solubility, a lack of synthetic methods for bigger cavity homologues and substituted CB[n], are limitations to the applicability of this family of hosts.¹¹⁻²⁰

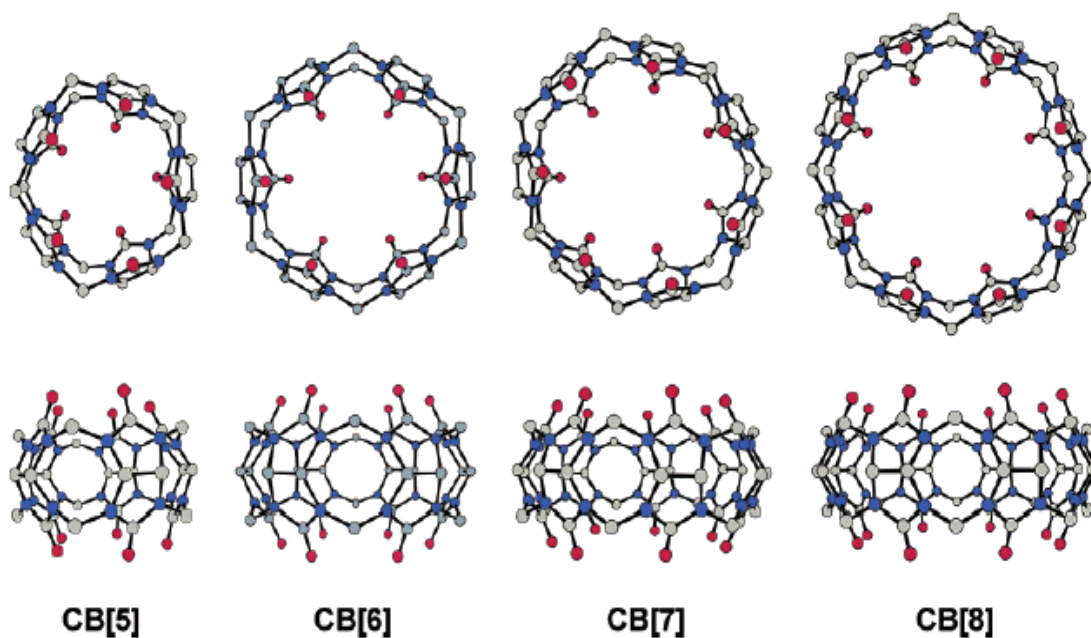


Figure 1.4 Non X-ray structure of the cucurbit[n]uril family.¹¹

The size of cucurbituril homologues is reported in Table 1.1. The cavity of CB[n] hosts is lipophilic and is suitable for binding a hydrophobic guest.

		CB[5]	CB[6]	CB[7]	CB[8]
outer diameter (Å)	a	13.1	14.4	16.0	17.5
cavity (Å)	b	4.4	5.8	7.3	8.8
	c	2.4	3.9	5.4	6.9
height (Å)	d	9.1	9.1	9.1	9.1
cavity volume (Å ³)	-	82	164	279	479

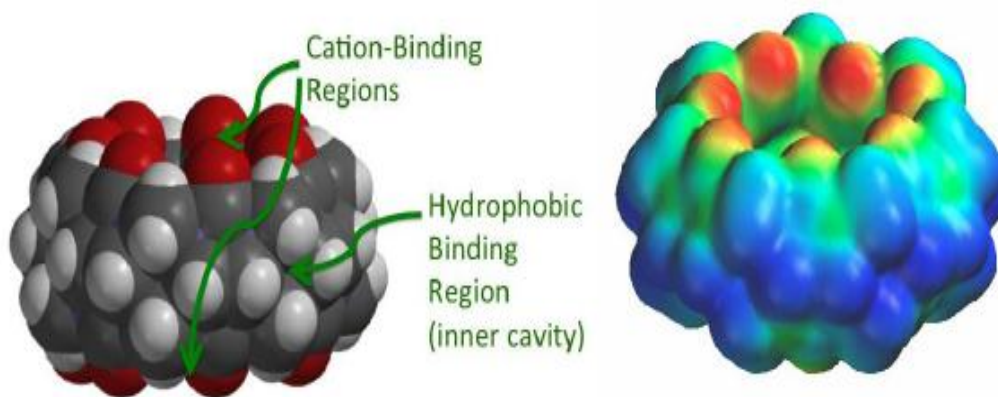
$n=5, 6, 7, 8$

Table 1.1 Parameters of cucurbit[n]urils family.¹¹

In addition, the carbonyl groups, which are on the lower and upper rims of CB[n] macrocycles are suitable for binding positively-charged guests by electrostatic interactions. The electrostatic potential profile of CBs show negative regions around the carbonyl groups and in the interior surface of the cavity; however, the outer surface is positive (Figure 1.5).

There are a variety of procedures for the synthesis of CB[n]; however, the most efficient and practical are those reported by Isaacs,²²⁻²³ Day,^{15-16, 21} and Kim.^{11, 13} As was mentioned before, the synthesis of all CB[n] is based on the acid-catalyzed condensation of glycoluril and formaldehyde (Figure 1.6). In view of the temperature of the reaction and/or type of acid used,

(a)



(b)

Figure 1.5 *The inner and external binding regions behavior (a), and the electrostatic potential surfaces of CB[7] (b).*^{7,11}

some homologues of CB[n] can be present as major or minor products. For instance, if the desired products are CB[5], CB[7] or CB[8], then the reaction temperature should be lowered to 75-90 °C. Next, the mixture of different CB[n] homologues is separated by

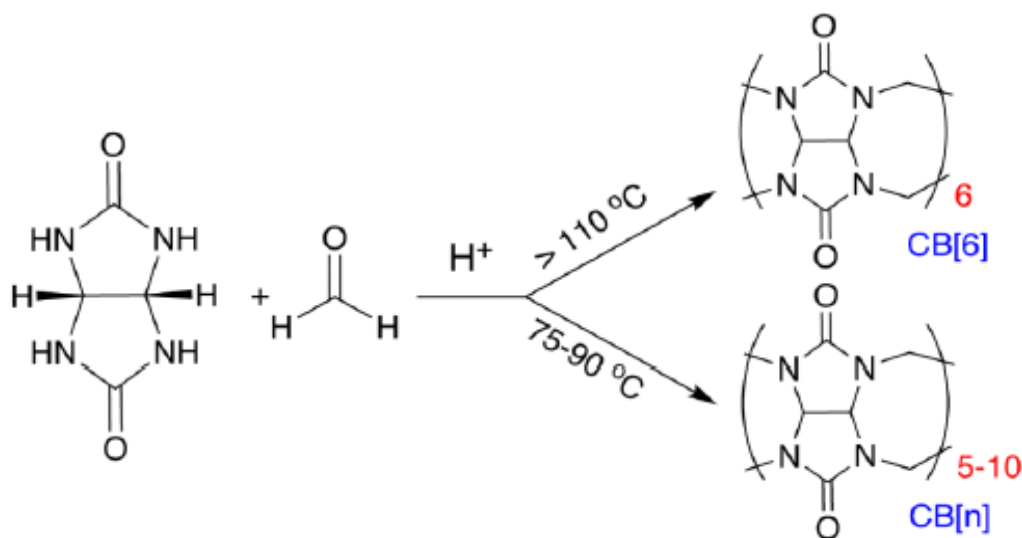


Figure 1.6 Pathways for CB[n] synthesis.^{7,11}

dissolution with acetone/ water, and fractional crystallization. Reaction temperatures higher than 110 °C will generate CB[6] as a major product. CB[n] are characterized by different analytical tools, such as: ¹H- NMR and mass spectrometry, as well as by X-ray crystallography.

The solubility of most CB[n] in most organic solvents and water is very low (<10⁻⁵ M), which is an important feature for their use as macrocyclic hosts. However, CB[5] and CB[7] are exceptions because they possess moderate solubility in water (2-3 x 10⁻² M).¹¹ Nevertheless, all CB[n] have good solubility in acidic water and in aqueous solutions of alkali metal ions because of the carbonyl portals, weak Lewis basicity and their affinity for interactions with cations (positively-charged species).^{7,11}

1.4 Cucurbit[7]uril as a host, its characteristics and application.

Cucurbit[7]uril (Figure 1.7) is the most frequently used homologue from the CB[n] family because of its relatively higher solubility in water and bigger cavity size (7.3 Å). These properties of CB[7] permit it to encapsulate a wider variety of guests (positively charged-cations, and neutral guests) by electrostatic interaction and due to its hydrophobic cavity. Also, the

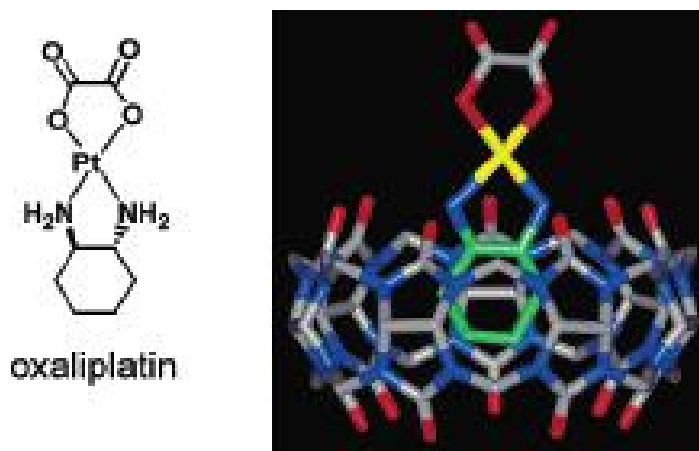


Figure 1.7 X-ray crystal structure of oxaliplatin/CB[7] complex.¹¹

carbonyl groups at the CB[n] portals are capable of coordination to metal ions. There are some known complexes of CB[7] which are formed with adamantanes,²⁴⁻²⁵ ferrocene,^{18,26-27} viologens,^{11,14} naphthalene,²⁹ stilbene,³⁰ nitroxide radicals;²⁸ and other guests.

The CB[7] complex with the dicationic methylviologen guest is very stable with a binding constant of $2.0 \times 10^5 \text{ M}^{-1}$, which was independently observed by both Kaifer¹⁴ and Kim.³⁰ The methylviologen; after a one-electron reduction, forms the species $\text{MV}^{+\cdot}$ (radical cation), which has a slightly lower binding constant than before ($\sim 1.0 \times 10$

$^5\text{M}^{-1}$). Upon a further one-electron reduction, the methylviologen species ($\text{MV}^{+\cdot}$) becomes the guest neutral form (MV^0) and it has a sharp decrease in its binding affinity to CB[7] (binding constant $\sim 2.0 \times 10^2 \text{ M}^{-1}$). This trend shows that the methylviologen binding affinity to CB[7] increases for the cationic-charged species of the guest, which electrostatically interacts with the electron-rich portals of CB[7] (C=O groups).¹¹

Recently, Kaifer and coworkers made an in-depth study of the influence of neutral and cationic guests on CB[7] complexes (Figure 1.8). As an example, they found that the presence of cations such as $\text{Na}^+(\text{NaCl})$ and $\text{Ca}^+(\text{CaCl}_2)$ can influence the encapsulation properties of $\text{CB}[7]@\text{MV}^{2+}$, resulting in the decrease of the complexation constant, which is $\sim 2.2 \times 10^5 \text{ M}^{-1}$ when no salt was added.³² They concluded that if the salt's concentration increases, most of the cations are competing with an encapsulated guest for binding with the electron-rich portals of the carbonyl groups on CB[7]. Therefore, the binding constant of methylviologen and CB[7] was widely decreased to $\sim 2.5 \times 10^4 \text{ M}^{-1}$ in the presence of NaCl and $\sim 5.6 \times 10^3 \text{ M}^{-1}$ when CaCl_2 was added.³²

Mock *et al.* demonstrated CBs cavity as a reaction chamber to mediate highly stereoselective chemical photoreaction of *trans*-diaminostilbenedihydrochloride (DAS).

³³ This work has shown that unstable species, such as DAS, can be stabilized by encapsulation inside CBs interior. The free *cis*-DAS can be changed to its unstable *trans*-DAS stereoisomeric form during UV light irradiation; however, in the dark, this reaction is reversible. On the other hand, if this *cis*-DAS forms a (1:1 H-G) complex with CB[7], the guest does not change its isomerization form at an appreciable rate at room temperature (Figure 1.9). From *ab initio* calculations, it is known that hydrogen bonds form with both terminal amine units of the *cis* isomer, with the electron-rich portal of

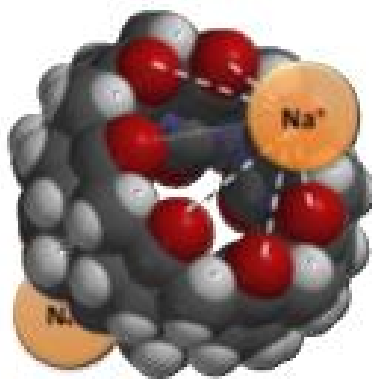


Figure 1.8 *Coordination of sodium ion to the portals of CB[7].⁷*

oxygens of CB[7] and results in a more stable complex. The cis isomer forms H- bonding on both ends of DAS resulting in a more stable complex.^{11, 33}

The influence of CB[7] on fluorescent enhancement of the guest during encapsulation, and explanation for the mechanisms of fluorescence quenching have been studied by Wagner, Nau and coworkers.³⁴⁻³⁶ For instance, encapsulation of 2,3-diazabicyclo [2.2.2]

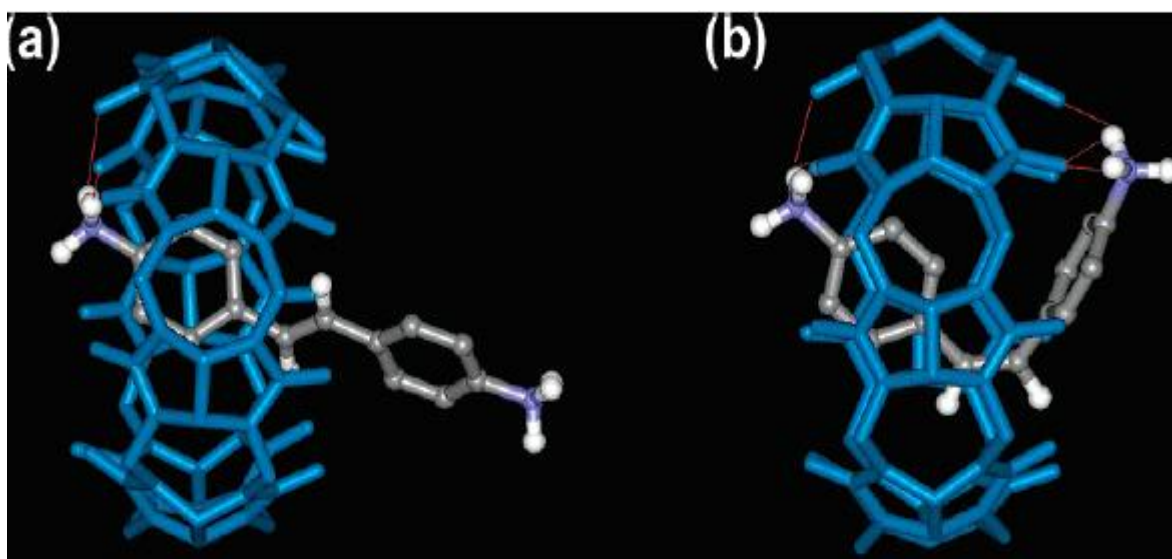


Figure 1.9 *Energy-minimized structures of (a) trans-DAS and (b) cis-DAS inside CB[7] cavity.¹¹*

octa-2-ene (DBO) inside the CB[7] increased the lifetime and the quantum yield fluorescence emission. This fact can be explained by CB[7]'s shielding of the fluorescent guest from quenchers such as oxygen. Additional advantages of binding fluorescent dyes inside CB[7] include decreased aggregation, and improved guest solubilization. This was shown for example for coumarin 102 and rhodamine 6G. The other important aspect of encapsulation is an enhancement of guest fluorescence, which can find application for the development of sensors. This effect was first observed by Wagner and coworkers in the encapsulation of curcumin with CB[7]: the complex emission intensity was five times higher than the free curcumin. Possibly this enhancement could be an effect of dye position in the hydrophobic interior of CB[7], restriction of conformation, or some H-G interaction. Additionally, when the fluorescent dye is enclosed within the CB[7] cavity it is "shielded" from reaction with external quenchers, reactants and oxidizers; therefore, it makes the encapsulated dye more photostable. This phenomenon offers the opportunity for numerous applications.³⁴⁻³⁶

Also, CB[7] was used as part of a sensor in enzyme assays for monitoring amino acid decarboxylases (important in tumor growth and inflammation) a method was developed by Nau and coworkers (Figure 1,10).³⁷⁻³⁸ They used Dapoxyl as a competitor because this fluorescence dye exhibits a stronger binding affinity for CB[7] than amino acid substrates. Nevertheless, after enzymatic cleavage of the amino acid carboxylate, the new decarboxylated product that is formed is able to displace the dye from CB[7] interior. In addition, the changes in the fluorescence signal of the dye (Dapoxyl), which is now free

after being encapsulated inside CB[7] cavity, easily gives proof that the dye was displaced by the substrate (dextracarboxylated amino acid).³⁷⁻³⁸

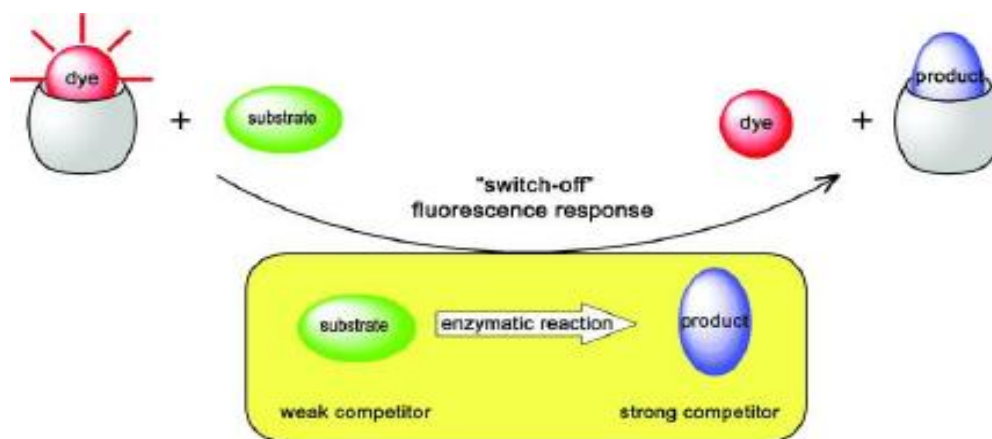


Figure 1.10 *Schematic view of the use of CB[7] as a sensor for enzyme assays.*³⁸

In summary, cucurbit[7]uril can be used for encapsulation of fluorescent or redox active compounds. Some useful applications include the use of CB[7] for catalyzing and inhibiting reactions, molecular switches and sensors, and in drug delivery to control release of drug.

1.5. Spectroscopic methods as tools used to identify and characterize H-G complexes properties.

Supramolecular H-G self-assembled systems can be characterized by a variety of analytical techniques, which include nuclear magnetic resonance (NMR) spectrometry, mass spectrometry (MS), UV- visible (UV-Vis) spectroscopy, fluorescence spectroscopy,

Fourier transform infrared (FT-IR) spectroscopy, Raman spectroscopy and X-ray crystallography. Some of these tools, such as NMR and UV-Vis spectroscopy are very helpful because they allow us to monitor the changes of host and guest spectroscopic properties upon complexation. Also, depending on H-G system, which is monitored and characterized by all of these tools, some important information about the encapsulated system can be found (such as: the binding constant, the location of the binding between H-G, their structures, and the stoichiometry of these systems).

NMR spectroscopy is the most versatile tool that is used for characterization in the H-G system study. The H-G complexation, which can be either a fast or slow exchange between bound and unbound host and guest molecules, can be detected by changes of chemical shift (δ) in NMR spectra (Figure 1.11 b).⁵ Changes in the shielding of protons, will result in changes of chemical shifts of the host and the guest. The monitoring of the chemical shift changes for the complexed or free guest can give additional information about formation of the H-G complex. The binding constant between the host and guest shows where these interactions take place by the location of nucleus and the regioselectivity of the guest binding (inside or outside of the host cavity). The NMR titration is based on collecting a series of spectra in which one component concentration (the host or guest) is constant and the concentration of the other is changed stepwise. Then, the binding constant of the H-G complex can be determined by plotting $\Delta\delta$ against added guest concentration, which suggests the stoichiometry in the H-G complex (relative percentage of the guest and the host in the solution; Figure 1.11 a).⁵

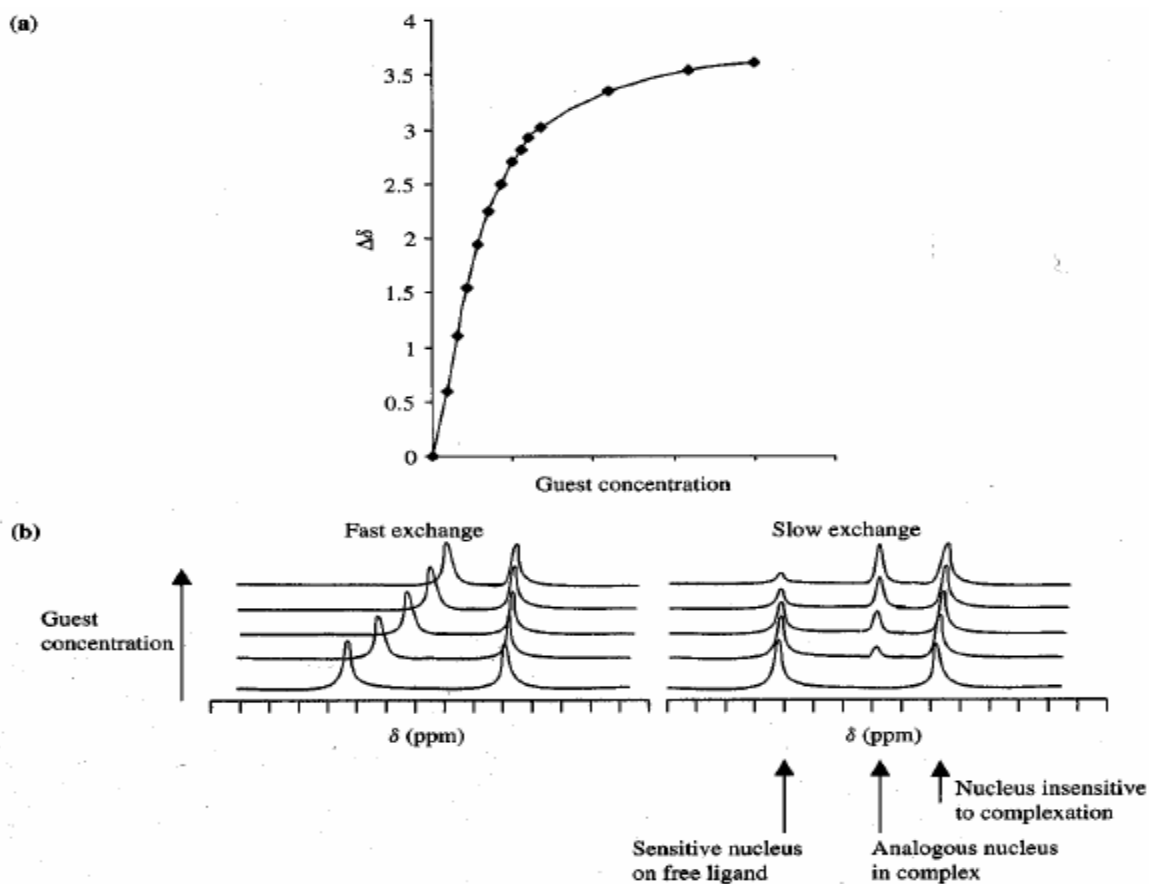


Figure 1.11(a) ^1H -NMR titration plot corresponding to fast exchange equilibration on the NMR time scale; and (b) Schematic NMR spectra of the guest fast and slow exchange equilibria.⁵

UV-Vis can also be an effective analytical technique; it is used for monitoring the encapsulation of the guest inside the host, and can be used as proof of complexation between the guest and host (UV-Vis titration).⁵ The UV-Vis titration involves keeping a constant concentration of the guest and changing of concentration of the host via its addition; this is recorded as changes of guest absorption (because bound and free guest absorbs UV-Vis light with different intensity and at different wavelengths). Then,

the changes of absorption are plotted against the host concentration, from which the binding constant of the H-G complex can be determined. Moreover, the correct stoichiometry of the H-G complex (the ratio of H:G) may be confirmed by a Job's plot, where changes of the H-G complex absorbance (ΔA) are plotted against concentration of $([Host]/[Host] + [Guest])$, which can be determined by the position of

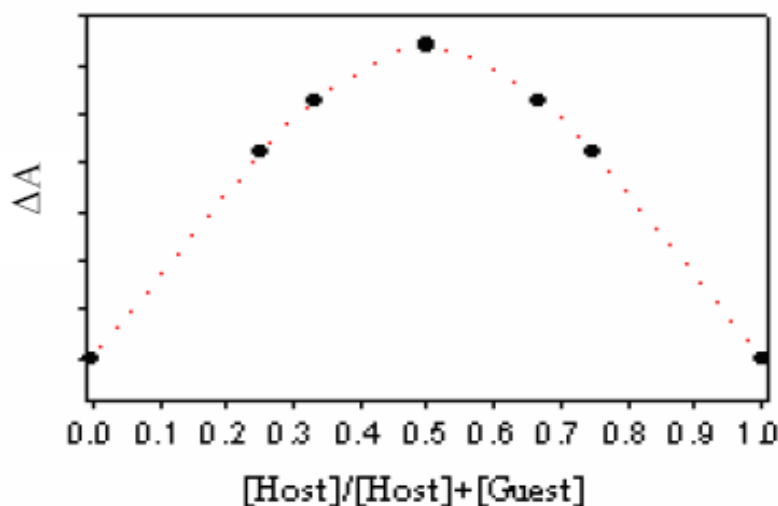


Figure 1.12 The UV-Vis Job's plot curve for a 1:1 host-guest complex.^{3,5}

the highest point. Thus, for the H-G complex of a 1:1 stoichiometry, a peak occurs at 0.5 (Figure 1.12), but for 2:1 it appears at 0.66.⁵

Mass spectrometry (MS) is another analytical tool, which provides important information about H-G complexes, such as their isotopic patterns, molecular weight and binding stoichiometry. There are different ionization methods, which are used in MS; however, since the H-G complex is formed by non-covalent interactions, soft ionization

methods are preferred. Electrospray ionization (ESI) or matrix- assisted laser desorption ionization (MALDI) are often used for this purpose.⁵⁸⁻⁵⁹

1.6 Properties of metal oxide nanoparticles (TiO_2 , ZrO_2).

In the last decades, nanostructured metal oxide nanoparticles because of their unique properties (such as a wide band-gap), have become very attractive for a large variety of

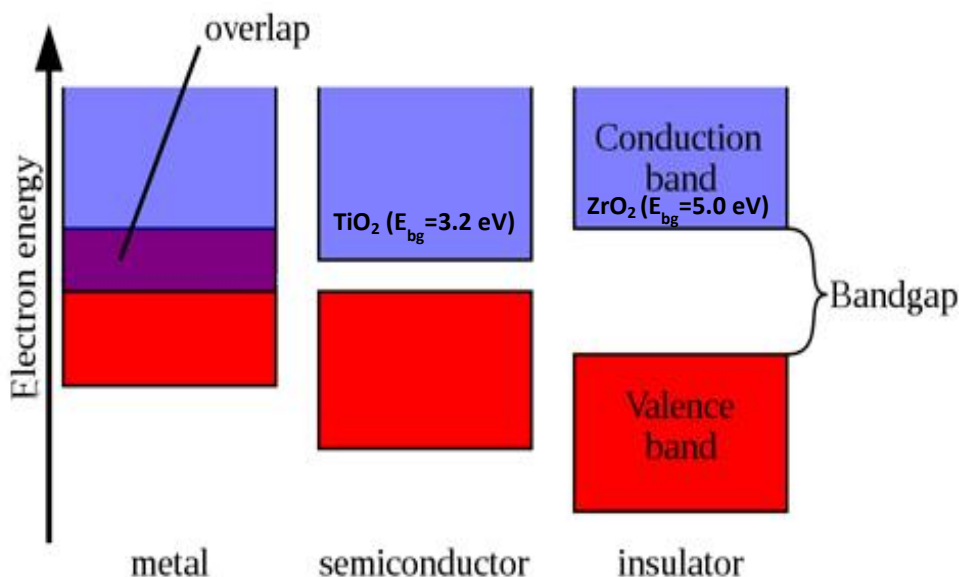


Figure 1.13 Differences in the band gaps.

applications, such as: sensors, photo-catalysis, electronic materials and photovoltaic devices (DSSCs -dye-sensitized solar cells). Depending on the band gap (E_{bg} – the energy difference between the conduction and valence band), metal oxide nanoparticles can be semiconductors or insulators (Figure1.13).

In this thesis we will focus on titanium dioxide (TiO_2) as n-type semiconductor with a wide band-gap, and compare its properties with another metal oxide nanoparticle, zirconium dioxide (ZrO_2), which is an insulator. The properties of TiO_2 and its applications are dependent on size, crystallinity, and morphology. Because of its low toxicity, good photocatalytic properties, chemical stability, and relatively low production cost, TiO_2 has been very popular for many scientific studies.

The term “nanoparticle”⁴¹ can be used to describe small objects such as a particle, or a number of atoms in a cluster, which size is classified in the nanometer scale (10^{-9} m). Mesoporous $\text{TiO}_2/\text{ZrO}_2$ films are good examples of (MO_n) nanoparticles. They are prepared by the sol-gel method (which will be described in Paragraph 2), but which involves hydrolysis and

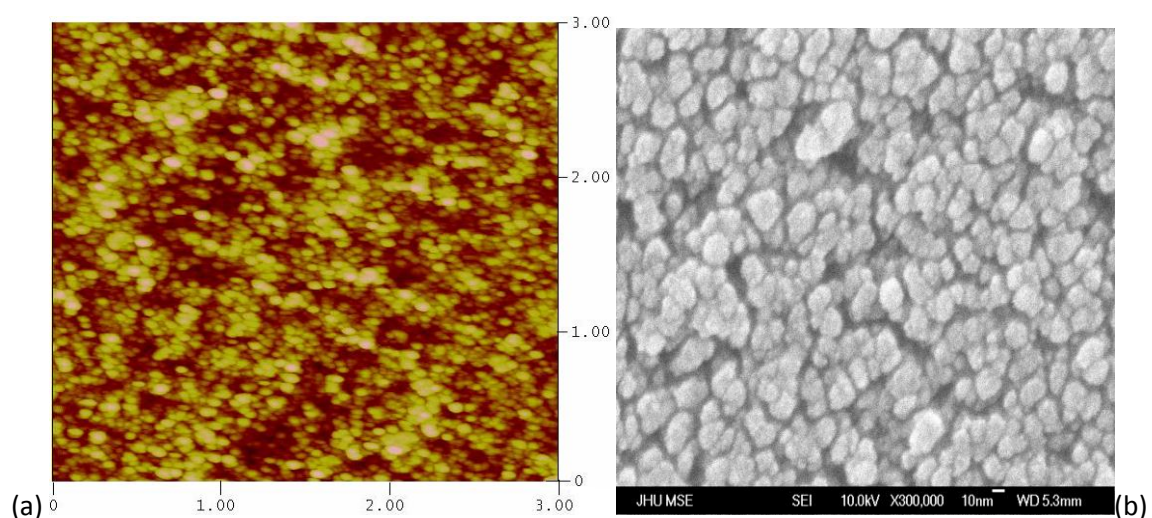


Figure 1.14(a) ATM image of TiO_2 film and (b) SEM image of ZrO_2 film.^{44, 60}

condensation of metal alkoxides in an alcoholic solution.⁷ Then, the $\text{TiO}_2/\text{ZrO}_2$ pastes are deposited on a conducting glass (FTO) and sintered at 450°C , which form a

filmcoating with optical transparency. Usually, the diameter of nanocrystalline $\text{TiO}_2/\text{ZrO}_2$ films has an average particle size~ 10-20 nm, and film thickness of 10 μm , which were determined by AFM and SEM (Figure 1.14).

TiO_2 (oxidation state IV) can exist in several crystalline forms, such as anatase (which exhibits better photoactivity), rutile and brookite. The band gap for anatase and rutile is known to be 3.2 and 3.0 eV, respectively, corresponding to an absorption threshold of 390-400nm. In view of these parameters TiO_2 has been studied as ideal photocatalyst used for water (Honda-Fujishima, 1972) ³⁹and air (CO_2 reduction)⁴⁰ purification applications. The photocatalytic process (Figure 1.15) is a consequence of the absorption of light of energy bigger than the band gap, during which electrons of the semiconductor's valence band are excited to the conduction band by forming electron-hole pairs. Then, the electron-hole recombination is suppressed by using a donor or an acceptor, which then trap the electrons.

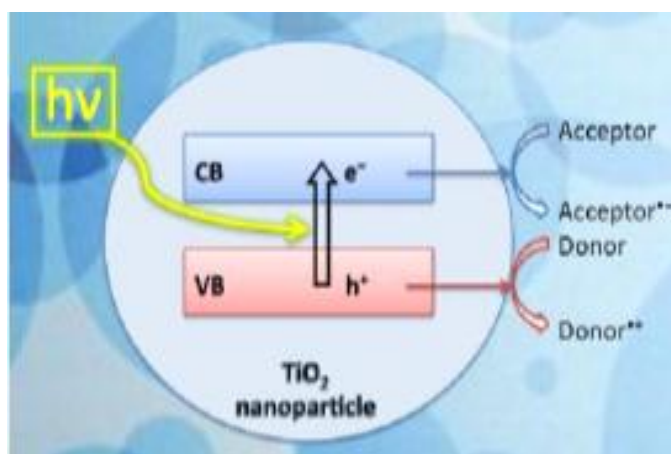


Figure 1.15 *The mechanism of charge separation in TiO_2 nanoparticle.*⁷

Zirconium dioxide (ZrO_2) nanoparticles have a morphology similar to TiO_2 , but ZrO_2 acts as an insulator because of its wide band gap ($E_{\text{bg}}=5-7$ eV depending on the crystal phase and preparation method); the threshold for absorption is at 300nm. Therefore, these properties make ZrO_2 nanocrystalline films very useful substrates to study the fluorescence emission of dyes bound to metal oxide nanoparticle surface, since fluorescence emission of the dye on ZrO_2 is not quenched.⁴²⁻⁴³

1.6.1 Binding H-G complexes to Metal Oxide surfaces.

Molecular functionalization of metal oxide (MO_n) interfaces with chromophores, redox and photoactive compounds (etc.), enables their use in various applications such as DSSC, photocatalysts, electrochromic devices, etc. The active compounds are attached to the MO_n films by covalent binding, physisorption, ion pair association, trapping in host and pores (H-G complexes) and by hydrophobic interactions. They are designed to have anchor groups such as $-\text{O}-\text{Si}-$, $-\text{SH}$, $-\text{P}(=\text{O})(\text{OH})_2$ or $-\text{COOH}$ that form a covalent bond

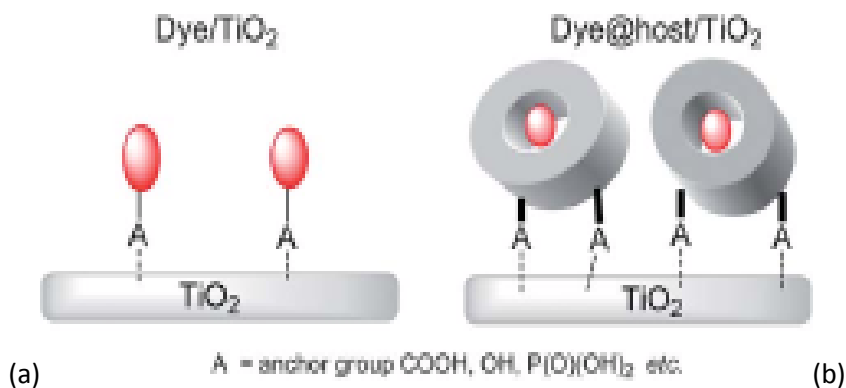


Figure 1.16 *Direct binding of the dye molecule (a) on the (MO_n) surfaces and (b) binding through encapsulation inside a host.*⁴⁵

with the (MO_n) semiconductor surface (Figure 1.16). Nevertheless, this molecular functionalization results in aggregation and uncertainty of the binding; for this reason, there has been a great effort to control binding through molecular design (for instance, use of rigid linkers).^{42, 45}

The encapsulation of the guest (dye) molecule inside the cavity of macrocyclic hosts (hemicarceplexes, cucurbiturils, cyclodextrins, calixarenes, etc.) is one recent and little explored strategy which enables one to bind the guest molecule trapped in the host to the surface of the semiconductor without modification of the guest with functional groups. If an encapsulated guest is able to create a stable complex with a host, the H-G complex may enhance the molecule's chemical, photophysical and electrochemical properties, as will be discussed in section 1.6.1. For instance, it can have advantageous effects, which can increase the dye stability and fluorescence lifetime or prevent aggregation and excited state quenching.⁴⁶⁻⁴⁸

There are examples of H-G complexes interacting on semiconductors surfaces, which were studied by Piotrowiak,⁴⁹⁻⁵⁰ Haque,⁵¹ Ko,⁵⁴ using hemicarceplexes and cyclodextrins as hosts to study the donor-acceptor charge transfer at interfaces.

In a pioneering study, the hemicarceplex interactions with nanoparticles of TiO_2 were studied by Piotrowiak and coworkers.⁴⁹⁻⁵⁰ The covalently bound complex of the chromophore (azulene) encapsulated inside a COOH -subtracted hemicarcerand, exhibited interfacial charge transfer in a hybrid assembly. They analyzed how encapsulated and free azulene dye can affect the charge transfer dynamics and compared the differences (Figure 1.17). The hemicarcerand host with its hydrophobic cavity was

suitable for encapsulating small organic dyes such as azulene forming a stable complex in aqueous solution; this was probed by $^1\text{H-NMR}$ and UV-Vis spectroscopy. Then, this complex was bound to colloidal TiO_2 nanoparticles, and FT-IR spectra were obtained by monitoring the changes in the C=O group stretching. The complex of Az@hemicarcerand (binding constant $1 \times 10^8 \text{ M}^{-1}$, quantum yield of 0.02 and a lifetime 1.5 ns) bound to TiO_2 has shown a rapid and efficient photoinduced electron transfer. The slow recombination kinetics was

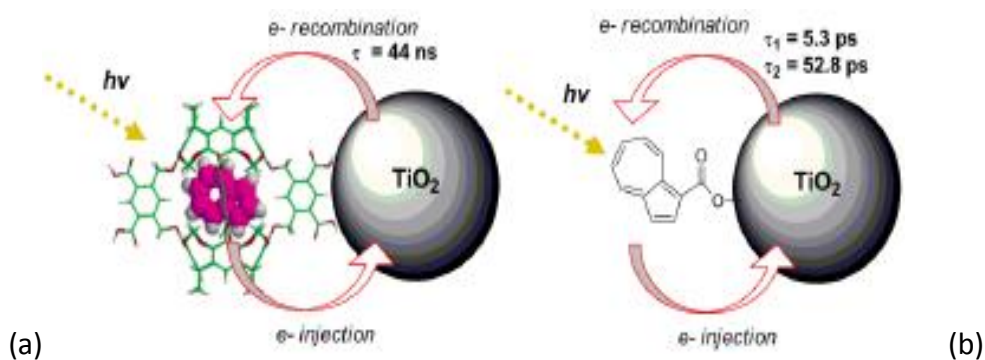


Figure 1.17(a) Charge transfer in the azulene@hemicarcerand complex bound to TiO_2 ; (b) comparison with free, directly bound dye.⁴⁹⁻⁵⁰

the consequence of slow tunneling of electrons through walls of the host. Finally, the encapsulated azulene attached to TiO_2 proved to be stable, very different than the free, directly-attached azulene which decomposed quickly. Therefore, the encapsulation of the dye by the host (as a H-G complex) improved its photo stability and resulted in slower charge recombination (two orders of magnitude) on a semiconductor surface.

From various sizes of macrocyclic hosts, cyclodextrins (CDs) are another host group that were used to functionalize semiconductor surfaces. The first who worked with CDs were Haque and coworkers,⁵¹ who used azobenzene dye encapsulated inside α -CD (capped

with bulky groups) for binding to TiO_2 surfaces. Their study focused on a comparison between the azobenzene@ α -CD complex ($1@ \alpha$ -CD) and azobenzene directly attached to TiO_2 films (Figure 1.18). The functionalized films of an encapsulated and directly bound azobenzene in both cases give the proof of binding to TiO_2 by monitoring the UV-Vis spectra of these films. In addition, similar as in the previous azulene complex, the $1@ \alpha$ -CD attached to TiO_2 has a slower charge recombination than the directly bound azobenzene dye ($\tau_{1/2} \sim 300$ and $4 \mu\text{s}$, respectively).

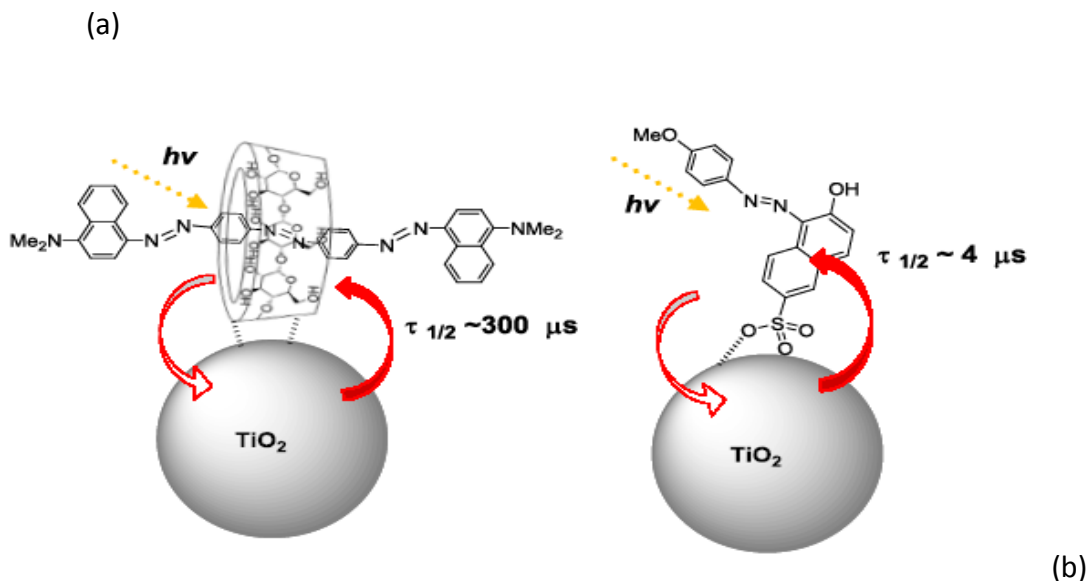


Figure 1.18(a) Suggested structure of azobenzene dye ($1@ \alpha$ -CD) complex and (b) directly bound azobenzene dye to TiO_2 .⁵²

Therefore, from these studies, it may be concluded that the interfacial charge transfer is controlled by the guest encapsulation inside the host interior. Another study, which is based on binding cyclodextrin complexes to TiO_2 films (and preparation of DSSCs devices), was done by Ko and coworkers.⁵⁴ During this research all homologues of cyclodextrin (α -, β -, γ -CD) were used to encapsulate the dye (JK-2) (3-{5' [NN-bis(9,9-

dimethylfluorene-2-yl)phenyl}-2,2'-bisthiophene-5-yl}-2-cyano-acrylic acid; then these complexes were attached to TiO_2 nanostructured films (Figure 1.19). Nevertheless, from the study it was observed that a JK-2@ β -CD complex had a marginally higher efficiency than other CDs homologues (DSSCs devices- Table 1.1).

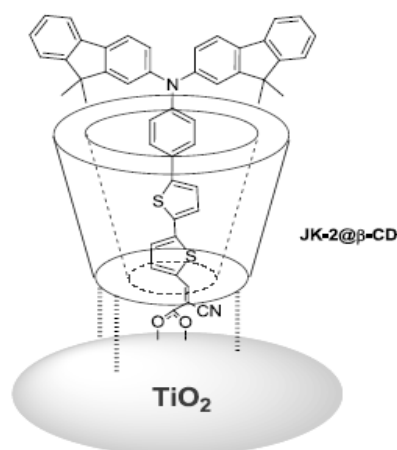


Figure 1.19 Proposed attachment of JK-2@ β -CD complex to TiO_2 surface.⁵⁷

Dye assembly	$J_{sc} V_{oc} ff_{\eta}$ [mAcm ⁻²] [V]	[%]		
JK-2	14.51	0.70	0.73	7.42
JK-2@ β -CD	15.34	0.76	0.74	8.65
JK-2@ α -CD	14.26	0.71	0.73	7.41
JK-2@ γ -CD	13.68	0.74	0.73	7.42

Table 1.2 Performance of DSSCs prepared from JK-2 dye.⁵⁴

The encapsulation of the JK-2 dye into β -CD as a kind of immobilization of the dye on TiO_2 film prevents aggregation of the dye and gives effective charge separation, which influences the delay of the interfacial charge recombination.⁵⁴

In conclusion, the molecular functionalization of metal oxide nanostructure surfaces (such as TiO_2) via covalent binding of H-G complexes to its surface prevents dye aggregation and in many cases significantly changes the properties of the dye encapsulated into the host; therefore, there are applications in many technological fields. This modification of the metal oxide nanoparticle surface with encapsulated dye inside the cavity of the host can enhance this particle's catalytic properties by interactions between a host and the semiconductor. Also, the H-G complex covalently bound on the (MO_n) surface prevents aggregation (stabilizes neighboring particles) and it may serve as electron donor to active metal catalyst.

REFERENCES

- (1) Lehn, J.-M. *Supramolecular Chemistry*, 1st ed.; VCH Verlagsgesellschaft mbH: Weinheim, **1995** pg 1-9.
- (2) Lehn, J.-M., *Angew. Chem. Int. Ed. Engl.* **1988**, 27, 89-112.
- (3) Yuan L.: Host-Guest Complexation Bases on Cucurbiturils.- thesis, **2008**.
- (4) Lee J. W., Samal S., Selvapalam N., Kim H.-J., Kim K.: Cucurbituril Homologues and Derivatives: New Opportunities in Supramolecular Chemistry. *Acc. Chem. Res.* **2003**, 36, 621-630.
- (5) Steed J., Atwood J.L.: *Supramolecular Chemistry*. John Wiley & Sons, **2009**.
- (6) Beer P.D., Gale P. A., Smith D. K.: *Supramolecular Chemistry*. Oxford Chemistry Primers, 74, Oxford University Press: Oxford, **2003**, pp. 1-14.
- (7) Fraitag M.: Host-Guest Chemistry Between Cucurbit[7]uril and Neutral and Cationic Guests.-thesis, **2011**.
- (8) Behrend, R.; Meyer, E.; Rusche, F. *Liebigs Ann. Chem.* **1905**, 339, 1.
- (9) Freeman, W. A.; Mock, W. L.; Shih, N.Y.: Cucurbituril. *J. Am. Chem. Soc.* **1981**, 103, 7367.
- (10) Mock, W. L.; Shih, N. Y.: Structure and Selectivity in Host-Guest Complexes of Cucurbituril. *J. Org. Chem.* **1986**, 51, 4440-4446.
- (11) Lee, J. W.; Samal, S.; Selvapalam, N.; Kim, H.-J.; Kim, K.: Cucurbituril Homologues and Derivatives: New Opportunities in Supramolecular Chemistry. *Accounts of Chemical Research* **2003**, 36, 621-630.
- (12) Kim, K.: Mechanically Interlocked Molecules Incorporating Cucurbituril and Their Supramolecular Assemblies. *Chem. Soc. Rev.* **2002**, 31, 96-107.
- (13) Kim, J.; Jung, I.-S.; Kim, S.-Y.; Lee, E.; Kang, J.-K.; Sakamoto, S.; Yamaguchi, K.; Kim, K.: New Cucurbituril Homologues: Syntheses, Isolation, Characterization, and X-ray Crystal Structures of Cucurbit[n]uril (n = 5, 7, and 8). *J. Am. Chem. Soc.* **2000**, 122, 540-541.
- (14) Kim, H. J.: Supramolecular Chemistry and Self-Assembly Special Feature: Inclusion of Methylviologen in Cucurbit[7]uril. *Proc. Nat. Acad. Sci.* **2002**, 99, 5007-5011.
- (15) Day, A.; Arnold, A.; Blanch, R.: A Method for Synthesizing Partially Substituted Cucurbit[n]uril. *Molecules* **2003**, 8, 74-84.
- (16) Day, A. I.; Blanch, R. J.; Arnold, A. P.; Lorenzo, S.; Lewis, G. R.; Dance, I.: A Cucurbituril-Based Gyroscane: A New Supramolecular Form. *Angew. Chem. Int. Edit.* **2002**, 41, 275-277.
- (17) Jeon, W. S.; Kim, H.-J.; Lee, C.; Kim, K.: Control of the Stoichiometry in Host-Guest Complexation by Redox Chemistry of Guests: Inclusion of Methylviologen in Cucurbit[8]uril. *Chem. Comm.* **2002**, 1828-1829.
- (18) Jeon, W. S.; Moon, K.; Park, S. H.; Chun, H.; Ko, Y. H.; Lee, J. Y.; Lee, E. S.; Samal, S.; Selvapalam, N.; Rekharsky, M. V.; Sindelar, V.; Sobransingh, D.; Inoue, Y.; Kaifer, A. E.; Kim, K.: Complexation of Ferrocene Derivatives by the Cucurbit[7]uril Host: A Comparative Study of the Cucurbituril and Cyclodextrin Host Families. *J. Am. Chem. Soc.* **2005**, 127, 12984-12989.
- (19) Kim, K.; Selvapalam, N.; Ko, Y. H.; Park, K. M.; Kim, D.; Kim, J.: Functionalized Cucurbiturils and Their Applications. *Chem. Soc. Rev.* **2007**, 36, 267.
- (20) Ko, Y. H.; Kim, E.; Hwang, I.; Kim, K.: Supramolecular Assemblies Built with

- Host-Stabilized Charge-Transfer Interactions. *Chem. Comm.* **2007**, 1305-1315.
- (21) Day, A.; Arnold, A. P.; Blanch, R. J.; Snushall, B.: Controlling Factors in the Synthesis of Cucurbituril and Its Homologues. *J. Org. Chem.* **2001**, *66*, 8094-8100.
- (22) Burnett, C. A.; Lagona, J.; Wu, A.; Shaw, J. A.; Coady, D.; Fettinger, J. C.; Day, A. I.; Isaacs, L.: Preparation of Glycoluril Monomers for Expanded Cucurbit[n]uril Synthesis. *Tetrahedron* **2003**, *59*, 1961-1970.
- (23) Lagona, J.; Mukhopadhyay, P.; Chakrabarti, S.; Isaacs, L.: The Cucurbit[n]uril Family. *Angew. Chem. Inter. Edit.* **2005**, *44*, 4844-4870.
- (24) Liu S., Ruspic Ch., Mukhopadhyay P., Chakrabarti S., Zavalij P.Y., Isaack L.: The Cucurbit[n]uril Family: Prime Components for Self-Sorting Systems. *J. Am. Chem. Soc.* **2005**, *127*, 15959-15967.
- (25) Hettiarachchi, D. S. N.; Macartney, D. H.: Cucurbit[7]uril Host-Guest Complexes *J. Chem.* **2006**, *84*, 905-914.
- (26) Cui, L.; Gadde, S.; Li, W.; Kaifer, A. E.: Electrochemistry of the Inclusion Complexes Formed Between the Cucurbit[7]uril Host and Several Cationic and Neutral Ferrocene Derivatives, A., A. Part of the Langmuir 25th Year: Molecular and Macromolecular Self-Assemblies, A Special Issue. *Langmuir* **2009**, *25*, 13763-13769.
- (27) Ong, W.; Kaifer, A. E.: Unusual Electrochemical Properties of the Inclusion Complexes of Ferrocenium and Cobaltocenium with Cucurbit[7]uril. *Organometallics* **2003**, *22*, 4181-4183.
- (28) Mileo, E.; Mezzina, E.; Grepioni, F.; Pedulli, G. F.; Lucarini, M.: Preparation and Characterisation of a New Inclusion Compound of Cucurbit[8]uril with a Nitroxide Radical. *Chemistry – A European Journal* **2009**, *15*, 7859-7862.
- (29) Wagner, B. D.; Stojanovic, N.; Day, A. I.; Blanch, R. J.: Host Properties of Cucurbit[7]uril: A Fluorescence Enhancement of Anilinonaphthalene Sulfonates. *J. Phys. Chem. B* **2003**, *107*, 10741-10746.
- (30) Choi, S.; Park, S. H.; Ziganshina, A. Y.; Ko, Y. H.; Lee, J. W.; Kim, K.: A Stable cis-Stilbene Derivative Encapsulated in Cucurbit[7]uril. *Chem. Comm.* **2003**, 2176-2177.
- (31) W. Ong, M. Gomez Kaifer, and A.E. Kaifer, *Org. Lett.*, **2002**, *4*, 1791.
- (32) Ong, W.; Kaifer, A. E.: Salt Effects on the Apparent Stability of the Cucurbit[7]uril, Methyl Viologen Inclusion Complex. *J. Org. Chem.* **2004**, *69*, 1383-1385.
- (33) Mock W. L., Irra T. A., Wepsiec J. P., Adhya M.: Catalysis by Cucurbituril. The Significance of Bound-Substrate Destabilization for Induced Triazole Formation. *J. Org. Chem.* **1989**, *54*, 5302-5308.
- (34) Nau, W. M.; Mohanty, J.: Taming Fluorescent Dyes with Cucurbituril. *Int. J. Photoenergy* **2005**, *7*, 133-141.
- (35) Praetorius, A.; Bailey, D. M.; Schwarzlose, T.; Nau, W. M.: Design of a Fluorescent Dye for Indicator Displacement from Cucurbiturils: A Macrocyclic-Responsive Fluorescent Switch Operating through a pKa Shift. *Org. Lett.* **2008**, *10*, 4089-4092.
- (36) Koner, A. L.; Nau, W. M.: Cucurbituril Encapsulation of Fluorescent Dyes. *Supramolecular Chemistry* **2007**, *19*, 55-66.
- (37) A. Hennig, H. Bakirci, and W.M. Nau, *Nat. Methods*, **2007**, *4*, 629.
- (38) Bailey D. M., Hennig A., Uzunova V.D., Nau V.D., *Chem. Eur. J.*, **2008**, *14*, 6069.
- (39) Fujishima, A.; Honda, K.: *Nature* **1972**, *238*, 37-38.

- (40) Roy S. C., Varghese O. K., Paulose M., Grimes C. A., *ACS Nano*. **2010**, 4, 637
- (41) Qi, W.; Wang, M.; Liu, Q.: Shape Factor of Nonspherical Nanoparticles. *J. Mat.Sci.* **2005**, 40, 2737-2739-2739.
- (42) Thyagarajan S., Galoppini E. Persson P., Giaimuccio J. M., Meyer G. J.: Large Footprint PyreneChromophores Anchored to Planar and Colloidal Metal Oxide Thin Films. *Langmuir* **2009**, 25, 9219-9226.
- (43) Rochford, J.; Galoppini, E.: Zinc(II) Tetraarylporphyrins Anchored to TiO₂, ZnO, and ZrO₂ Nanoparticle Films Through Rigid-Rod Linkers. *Langmuir* **2008**, 24, 5366-5374.
- (44) Fujishima, A.; Honda, K.: *Nature* **1972**, 238, 37-38.
- (45) Freitag M, Galoppini E.: Molecular Host-Guest Complexes: Shielding of Guests on Semiconductor Surfaces. *Energy Environ. Sci.* **2011**, 4, 2482-2494.
- (46) Lehn, J. M.; Atwood, J. L.; Suslick, K. S.; Davies, J. E. D.; Macnicol, D. D.; Vogtle, F.: *Comprehensive Supramolecular Chemistry: Supramolecular Reactivity and Transport-Bioinorganic Systems*. Elsevier Science Ltd. **1999**.
- (47) Kamat, P. V.: Meeting the Clean Energy Demand: Nanostructure Architectures for Solar Energy Conversion. *J. Phys. Chem. C* **2007**, 111, 2834-2860.
- (48) Porel M., Klimczak A., Freitag M, Galoppini E., Ramamurty V.: Photoinduced Electron Transfer Across a Molecular Wall: Coumarin Dyes as Donors and Methyl viologen and TiO₂ as Acceptors. *Langmuir* **2012**, 28, 3355-3359.
- (49) Piotrowiak, P.; Deshayes, K.; Romanova, Z. S.; Pagba, C.; Hore, S.; Zordan, G.; Place, I.; Farrán, A.: Electron and Excitation Transfer in Hetero-Supramolecular Assemblies and at Molecule-Nanoparticle Interfaces. *Pure Applied Chemistry* **2003**, 75.
- (50) Pagba, C.; Zordan, G.; Galoppini, E.; Piatnitski, E. L.; Hore, S.; Deshayes, K.; Piotrowiak, P.: Hybrid Photoactive Assemblies: Electron Injection from Host-Guest Complexes into Semiconductor Nanoparticles. *J. Am. Chem. Soc.* **2004**, 126.
- (51) Haque, S. A.; Handa, S.; Peter, K.; Palomares, E.; Thelakkat, M.; Durrant, J. R.: Supermolecular Control of Charge Transfer in Dye-Sensitized Nanocrystalline TiO₂ Films: Towards a Quantitative Structure-Function Relationship. *Angew. Chem. Int. Edit.* **2005**, 44, 5740-5744.
- (52) Yang, D.-H.; Ju, M.-J.; Maeda, A.; Hayashi, K.; Toko, K.; Lee, S.-W.; Kunitake, T.: Design of Highly Efficient Receptor Sites by Combination of Cyclodextrin Units and Molecular Cavity in TiO₂ Ultrathin Layer. *Biosensors and Bioelectronics* **2006**, 22, 388-392.
- (53) Ju, M.-J.; Yang, D.-H.; Lee, S.-W.; Kunitake, T.; Hayashi, K.; Toko, K.: Fabrication of TiO₂ / γ -CD Films for Nitro Aromatic Compounds and its Sensing Application via Cyclic Surface-Polarization Impedance (cSPI) Spectroscopy. *Sensors and Actuators B: Chemical* **2007**, 123, 359-367.
- (54) Choi, H.; Kang, S. O.; Ko, J.; Gao, G.; Kang, H. S.; Kang, M.-S.; Nazeeruddin, M. K.; Grätzel, M.: An Efficient Dye-Sensitized Solar Cell with an Organic Sensitizer Encapsulated in a Cyclodextrin Cavity. *Angew. Chem. Int. Edit.* **2009**, 48, 5938-5941.
- (55) Katz, A.; Da Costa, P.; Lam, A. C. P.; Notenstein, J. M.: *Chem. Mater.* **2002**, 14, 3364.
- (56) Notenstein, J. M.; Iglesia, E.; Katz, A.: *Chem. Mater.* **2007**, 19, 4998.

- (57) Islam, A.; Sugihara, H.; Yanagida, M.; Hara, K.; Fujihashi, G.; Tachibana, Y.; Katoh, R.; Murata, S.; Arakawa, H.: Efficient Panchromatic Sensitization of Nanocrystalline TiO₂ Films by [small beta]-Diketonato Ruthenium Polypyridyl Complexes. *New Journal of Chemistry* **2002**, 26, 966-968.
- (57) Molenveld, P.; Engbersen, J. F. J.; Reinhoudt, D. N.: Dinuclear Metallophosphodiesterase Models: Application of Calix[4]arenes as Molecular Scaffolds. *Chem. Soc. Rev.* **2000**, 29, 75-86.
- (58) C.A. Schalley, *Int. J. Mass Spec.* **2000**, 194, 11.
- (59) C.A. Schalley, *Mass Spec. Rev.* **2001**, 20, 253.
- (60) Rebecca, J.; et al.: Transition Metal-Doped TiO₂ and ZnO, A Present Status of the Field. *J. Phys.: Condensed Matter* **2005**, 17, R657.

Chapter Two

Modification of TiO_2 Surface by Attachment

of Hemirhodopsin (the C-153@OA₂ Complex):

Photoinduced Electron Transfer Between C-153 and TiO_2

Introduction

In the past few decades, photoinduced electron transfer from an organic dye molecule to the conduction band of wide band-gap of metal oxide surfaces has attracted the interest of many scientific groups worldwide.¹⁻⁵ This process has been used for a variety of applications, such as: photocatalysis,¹⁵⁻¹⁶ molecular electronics,¹⁷ sensors¹⁸⁻¹⁹ and Dye-Sensitized Solar Cells (DSSCs).¹⁻² Most of the studies focus on modification of semiconductor surfaces by attaching many different organic dyes onto a variety of metal oxide surfaces, including TiO₂, ZnO and ZrO₂ (considered an insulator). TiO₂ is a semiconductor (see Section 1.6) with a large band-gap (3.2eV) and which absorbs only 3% of total solar radiation.⁶ Therefore, it is important to bind to it a dye with a wide absorption spectrum in the visible region and a very fast injection of the photoexcited electrons into TiO₂.^{6,11} There are numerous examples of ruthenium-based dyes and porphyrins exhibiting excellent conversion efficiency in DSSCs.⁸⁻¹⁰ Organic chromophores, such as coumarins,^{6-7,20} anthracene,²¹ pyrene,²² and other conjugated organic dyes can also be used in DSSCs. For instance, Coumarin 153 (C-153), because of very fast electron injection into the TiO₂ conduction band and a relatively high injection quantum yield (~90%), has been employed in DSSCs.¹²⁻¹³ Also, it is amenable to structural modifications: an electron-accepting substituent (trifluoromethyl group induces a big shift of the absorption from 365 to 430nm) shifts fluorescence maximum towards

Important note: Some of the sentences within this paragraph of this thesis were cited verbatim or slightly modified from the paper of which I am a co-author.⁷

low energy.⁶ However, the successful use of coumarins and many organic dyes which are used as electron donors/acceptors is often hampered because of their tendency for aggregation (a limitation of use as a sensitizer)^{7,20,23} and photodegradation.⁷ The encapsulation of the guest (organic dye) inside a macrocyclic host cavity (as a H-G complex) and attachment of this complex into metal oxides have been recently proposed as suitable methods for modification of semiconductor surfaces; these can overcome most of the problems. In addition, encapsulation not only prevents aggregation of the organic dye (guest), but results in dramatic differences in the injection and recombination processes changing the mechanism of interfacial electron transfer, and slowing the charge recombination rates.¹⁴

In recent years, Ramamurthy and coworkers have published photophysical

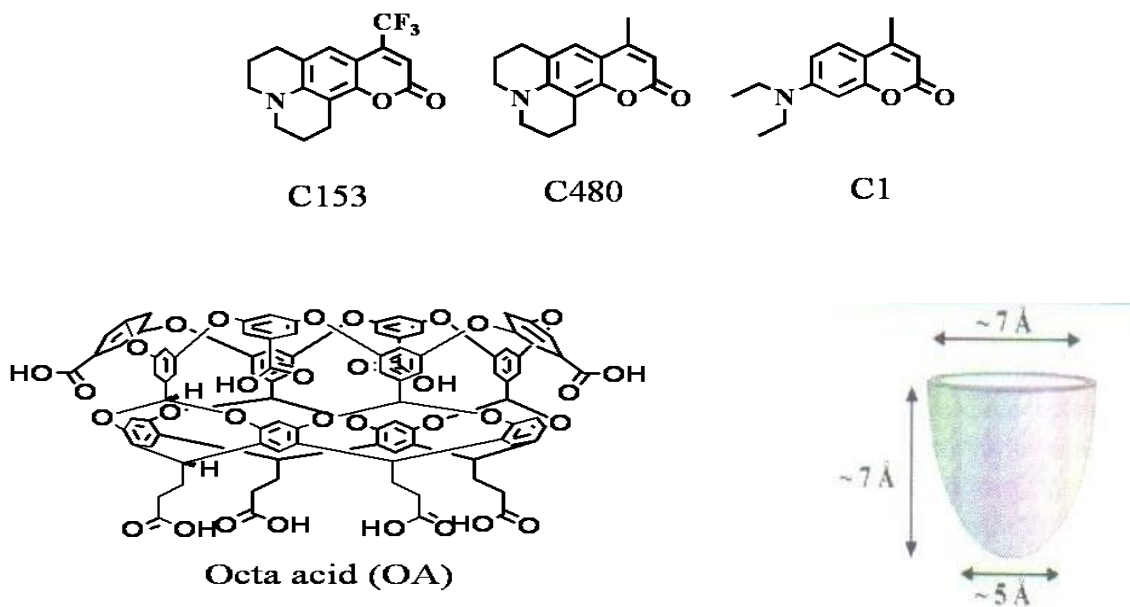


Figure 2.1 Structures of Host and Guest Molecules.⁷

and photochemical solution behavior of organic dyes encapsulated within two molecules of octa acids (Figure 2.1)²⁴⁻²⁷ From these studies, it is known that octa acid, with a

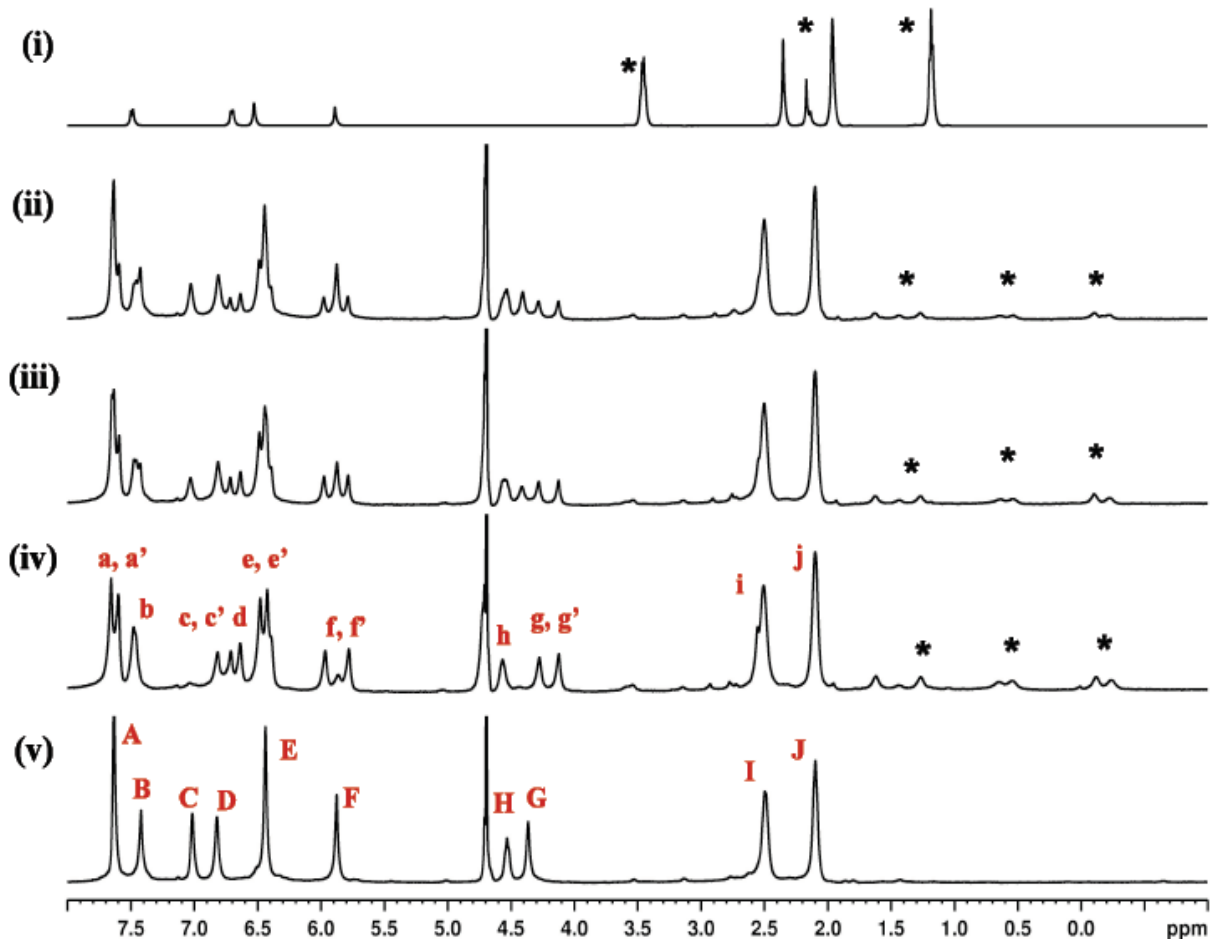


Figure 2.2 ^1H -NMR spectra of (i) C-153 in CD_3CN ; (ii)-(iv) C-153 in presence of OA at various guest: host ratios (by fixing host concentration and increasing guest concentration stepwise)(ii)C-153@OA (1:8) [C-153]=0.125 mM (iii) C-153@Oa (1:4) [C-153]=0.25 mM (iv) C-153@OA (1:2) [C-153]=0.5 mM (v) 1 mM OA in 10 mM buffered D_2O alone. A-J represents un-complex OA protons signals; a, a'-j represent complexed OA proton signals, and * represents the guest proton signals.²⁴

volume of 500 \AA^3 , forms a capsule (a G-H complex) by assembling two molecules of the host and one or two molecules of the guest.²⁷⁻²⁸ The ^1H -NMR spectra for complexes of

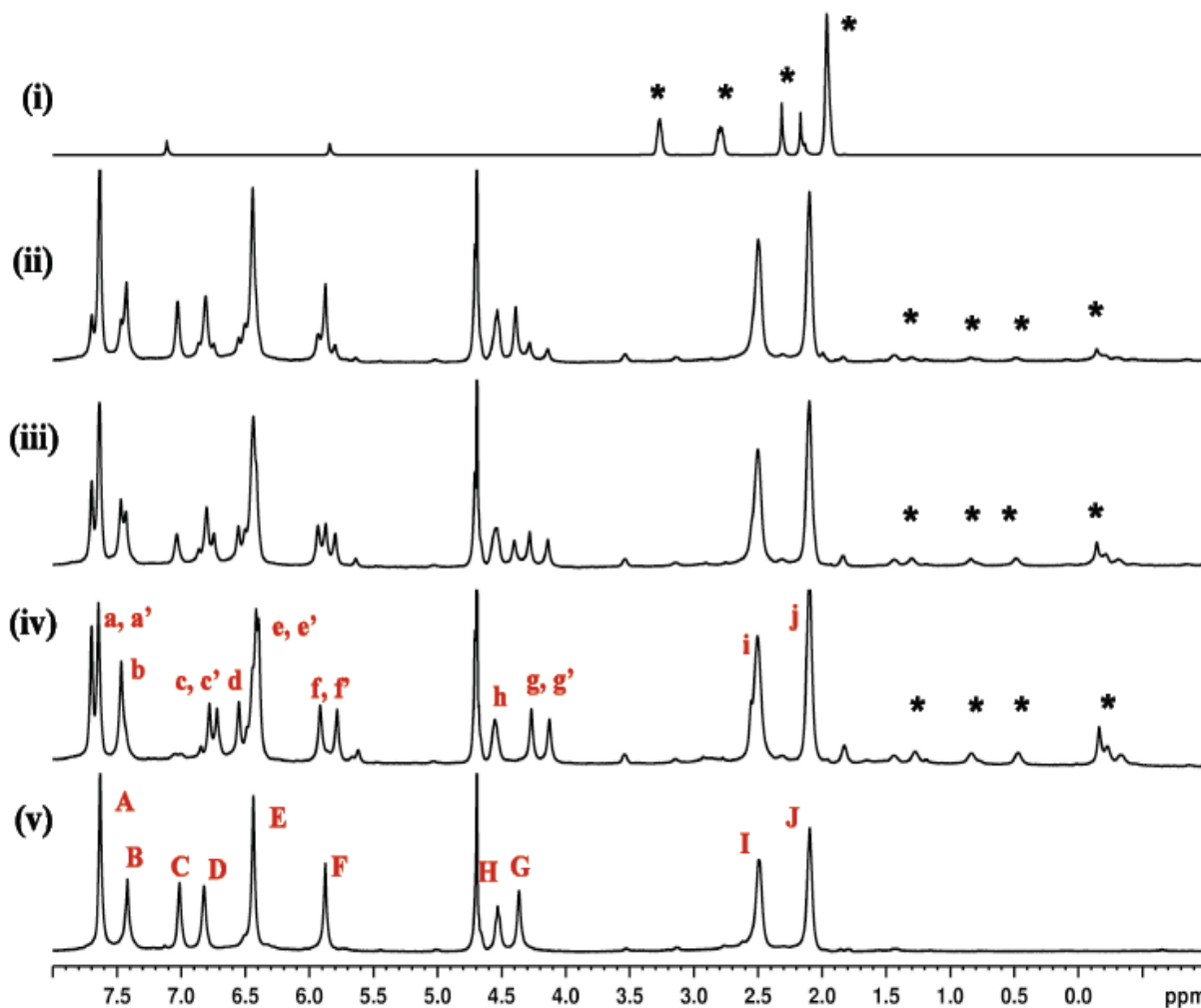
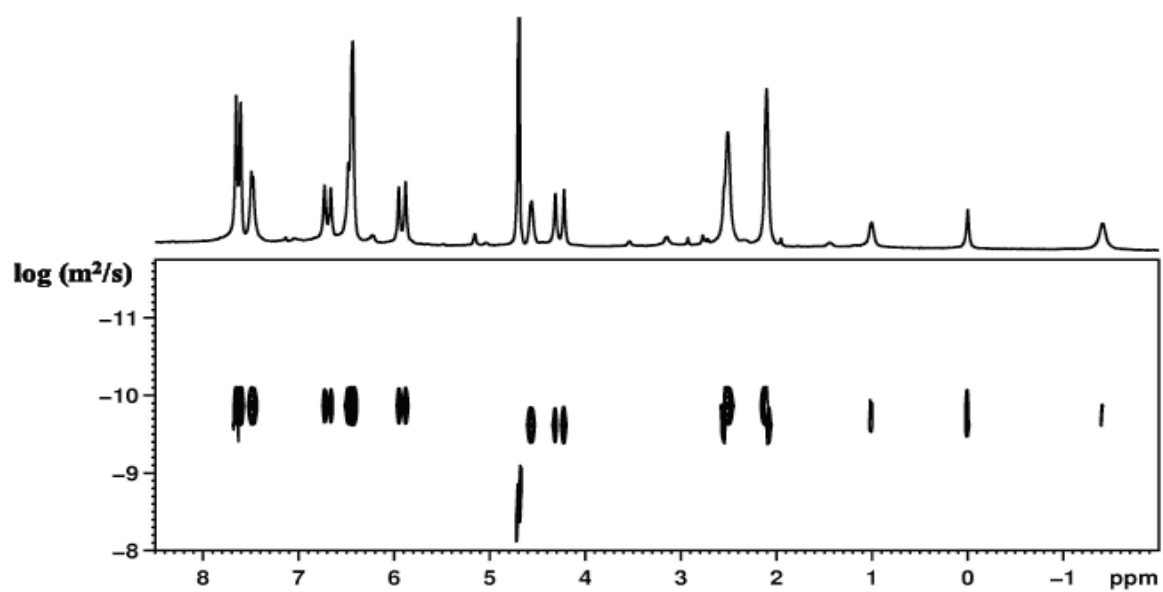
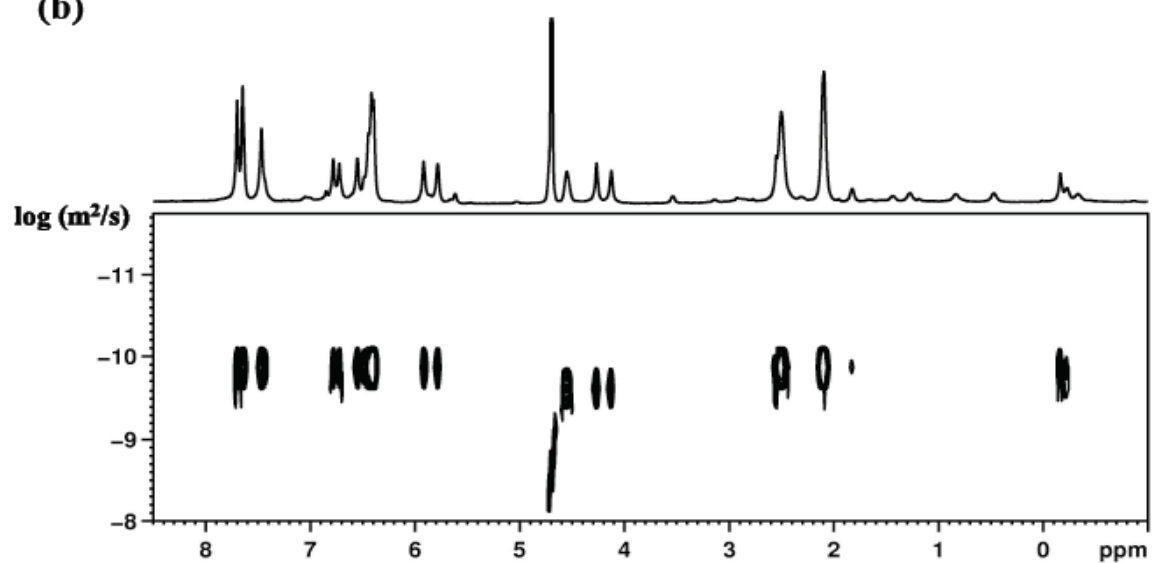


Figure 2.3 ^1H -NMR spectra of (i) C-480 in CD_3CN ; (ii)-(iv) C-480 in presence of OA at various guest: host ratios (by fixing host concentration and increasing guest concentration stepwise) (ii) c-480@OA (1:8) $[\text{C-480}] = 0.125 \text{ mM}$ (iii) C-480@OA (1:4) $[\text{C-480}] = 0.25 \text{ mM}$ (iv) C-480@OA (1:2) $[\text{C-480}] = 0.5 \text{ mM}$ (v) 1 mM OA in 10 mM buffered D_2O alone. A-J represents un-complexed OA proton signals; a,a'-j represent complexed OA proton signals, and * represents the guest proton signals.²⁴

OA with C-153, C-480, and C-1 were also established by the Ramamurthy group (Figure 2.2-2.3).²⁴ Thus, from this data it is known that all of these dyes form 1:2 (G-H complexes) capsules with OA in sodium tetraborate buffer solution (pH ~ 9). Moreover, DOSY NMR of these complexes (Figure 2.4) indicates that the host and the guest molecules are associated at the NMR time scale because molecules of the guest and the host possess identical diffusion constants ($\sim 1.25 \times 10^{-6} \text{ cm}^2/\text{s}$).

In our study, we focused on coumarins: C-1, C-153 and C-480 as donor dyes with long excited-state lifetimes (4-7.5 ns); these were chosen as suitable for encapsulation inside the water-soluble octa acid (OA, a carboxylic acid substituted with eight COOH groups at the periphery), and testing the photoinduced electron transfer to TiO₂ nanoparticle surfaces. Out of these three dyes, only C-153 can be selectively excited in the presence of TiO₂ because the UV-Vis absorption of C-153 is not overlapping with the absorption of TiO₂; ⁷ therefore, this thesis will focus on C-153.⁷ The illustration of all molecules of organic

(a)**(b)**

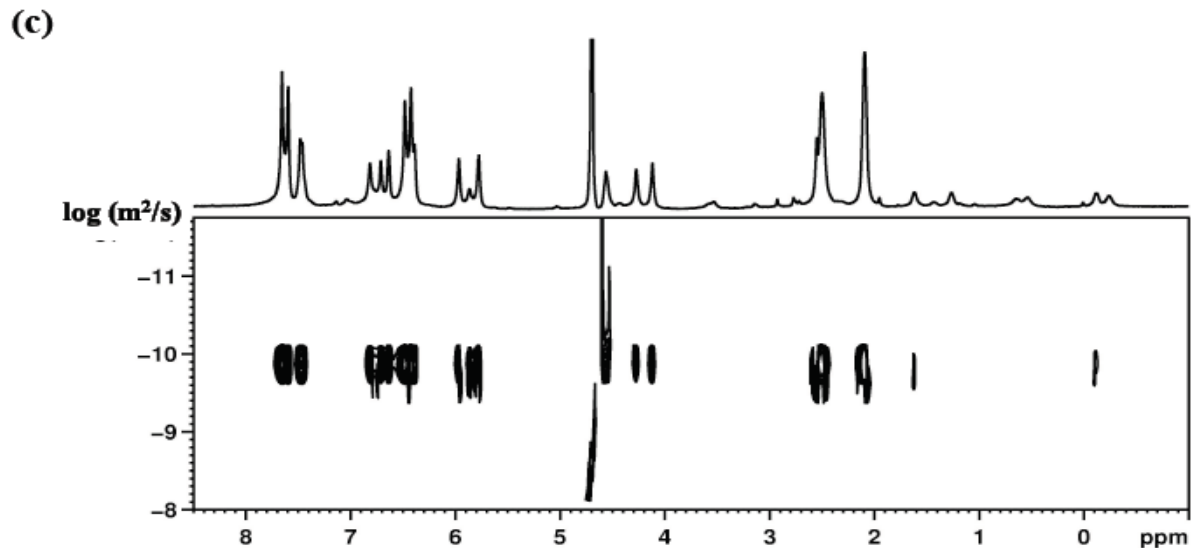


Figure 2.4 DOSY NMR spectra of (a) $C-1@OA_2(1:2)$; (b) $C-480@OA_2(1:2)$ and (c) $C-153@OA_2(1:2)$ complexes. $[OA] = 1\text{ mM}$ in 10 mM buffer D_2O and $[C-1; C-480; C-153] = 0.5\text{ mM}$.²⁴

dyes and a microcyclic host are shown in Figure 2.1.

Experimental Section

2.1. General.

The host, octa acid (OA), was synthesized by Ramamurthy group following the previously published procedure.²⁸ Laser grade dyescoumarin 1 (C-1), coumarin 153 (C-153) and coumarin 480 (C-480) were used as received from Sigma-Aldrich/Acros. The chemicals for TiO_2/ZrO_2 , such as 2-propanol, titanium (IV) isopropoxide, zirconium (IV) propoxide, nitric acid (ACS grade), and polyethylene glycol (av. Mol. Wt. 2,000) were used as received from Aldrich, Sigma –Aldrich and Fischer. Fluorescence emission

spectra of functionalized $\text{TiO}_2/\text{ZrO}_2$ films with the C-153@OA₂ complex (at pH7) binding onto their surfaces were recorded on a Cary Eclipse, Varian fluorescence spectrometer. All fluorescence spectra were collected at $\lambda_{\text{ex.}}=420$ nm. Before the spectroscopic measurements, all films were heated at 110°C in an oven for 30 minutes to remove moisture. Attenuated Total Reflectance Infrared (FT-IR-ATR) and Fourier Transform Infrared (FT-IR) spectra of OA (solid) and $\text{TiO}_2/\text{ZrO}_2$ films modified with C-153@OA₂ complex (at pH7) were obtained at room temperature on a Thermo Scientific Nicolet 6700 spectrometer (Zn-Se crystal) using 100 scans and a resolution of 4 cm^{-1} . The films were dried by heating in an oven at 110°C for 30 minutes before their measurements.

2.1.1 pH adjustment.

The adjustment of C-153@OA₂ pH was done by addition of aqueous HCl dropwise to the complex in aqueous sodium tetraborate buffer solution (pH~9). Then, the emission of the complex solution was recorded. From the data, it was observed that the λ_{max} of complex emission was almost same upto pH~7 (Figure 2.7 a). Upon further acid addition (pH<7) λ_{max} was redshifted and the intensity decreased, indicating decomplexation of C-153 from OA capsule. Therefore, for the binding study of the C-153@OA₂ complex on TiO_2 , pH7 was used.

2.1.2 TiO_2 and ZrO_2 synthesis.

Synthesis of $\text{TiO}_2/\text{ZrO}_2$ nanoparticle gels followed by hydrolysis of titanium(IV) isopropoxide/ zirconium(IV) propoxide in an aqueous nitric acid solution under nitrogen atmosphere. For set up were used: a three-necked round bottom flask with Dean-Stark

apparatus, dropping funnel (middle neck) and a thermometer (Figure 2.5). The three-necked round bottom flask, containing 100 mL solution of acidic water (0.69 mL of conc.-68-70%- HNO_3), was stirred vigorously at room temperature. Then, a mixture of 20 mL of titanium(IV) iso-propoxide/ zirconium(IV) propoxide with 80 mL of isopropanol (a total volume of 100 mL) was placed in the additional funnel, and purged with nitrogen for 10 min. The mixture was added through the dropping funnel to the acidic solution at the rate not faster than one drop per second. The immediate formation of a white precipitate in the flask indicated rapid hydrolysis of titanium(IV) iso-propoxide/ zirconium(IV) propoxide. During this addition, the reaction was kept stirring vigorously

Important note: I followed the procedure of $\text{TiO}_2/\text{ZrO}_2$ synthesis which was published before by our group;²⁹⁻³⁰ therefore, some of the sentences were slightly modified.

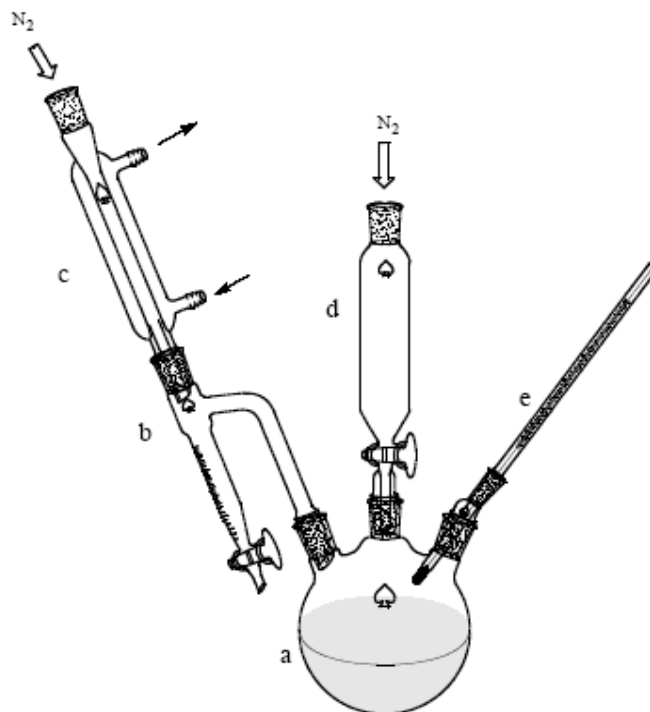


Figure 2.5 *The experimental set-up for the synthesis of $\text{TiO}_2/\text{ZrO}_2$.*²⁹

to prevent sticking of the particles to the flask. After the addition was completed, the dropping funnel was replaced with a stopper, and the reaction flask together with the Dean-Stark apparatus was covered by aluminum foil. The reaction mixture was brought to reflux, and an isopropanol/ water mixture (approximately 130 mL) was removed from the reaction solution at a temperature range of 86-95°C.

All isopropanol has been removed when the reflux temperature reaches 100°C, and the Dean-Stark apparatus was replaced with a reflux condenser. Then, the reaction mixture was kept at reflux overnight. Following the reflux, the three-neck round bottom flask was left opened. The reaction volume was reduced to 45 mL (TiO_2)/ 30mL (ZrO_2) by evaporation of the water, and allowed to cool down. Next, the white colloidal sol gel was

sonicated for 5 min, and transferred to an autoclaved glass beaker with a magnetic stirring rod. The beaker was placed into the titanium autoclave (Model 4760, Parr-Figure 2.6), and heated at 200°C for 12 h (at pressure 17-18 bar).

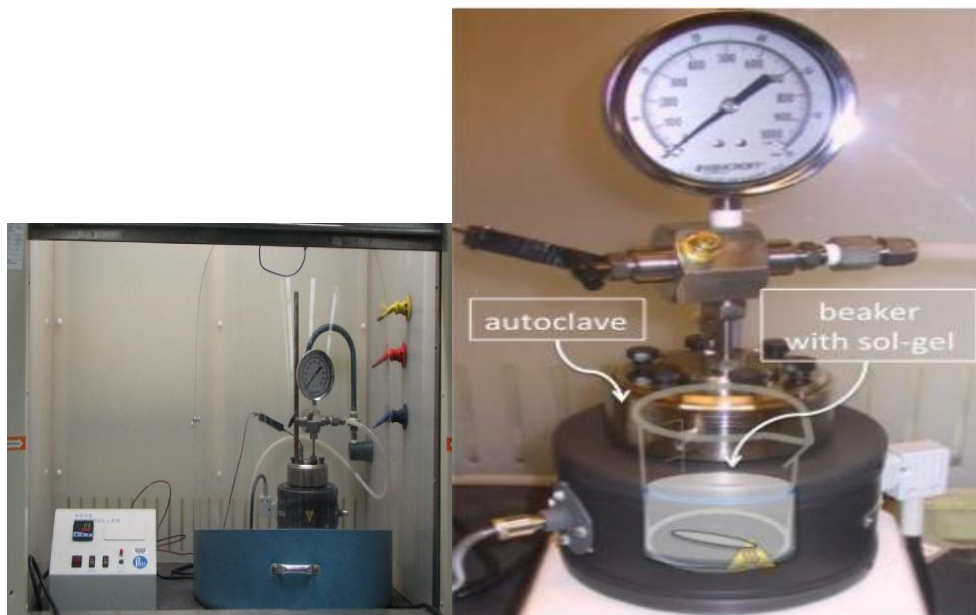


Figure 2.6 *The picture of the titanium autoclave for $\text{TiO}_2/\text{ZrO}_2$ nanoparticle colloids processes.*²⁹

The sol was allowed to cool to room temperature, and transferred from the autoclave beaker to a graduated beaker. The percentage weight of TiO_2 in the gel was determined via the ‘glass dies’ method, which involves weighing a small amount (one drop) of the gel on a glass before and after drying at 100°C for water removal. Then, from the difference, the wt. % of TiO_2 in the sol-gel was determined (it should be in a range of 13-17 wt. %). Polyethylene glycol (PEG 2,000; amount: 6g/100 mL) was added to the nanoparticle gel to optimize the solution viscosity and required uniform thickness of the films. The mixture was allowed to stir for approximately 72 h to guarantee a good

uniform gel. The nanoparticle $\text{TiO}_2/\text{ZrO}_2$ pastes were left covered from light exposure and were stored up to one month for thin film preparation, or until a yellow discoloration appears, which means degradation, so it should be discarded.

2.1.3 $\text{TiO}_2/\text{ZrO}_2$ films preparation and binding of the C-153@ OA_2 complex to the films.

The preparation of $\text{TiO}_2/\text{ZrO}_2$ films was done via the paste being spread on the conducting glass (FTO) by using a glass test tube and holding the edge of the glass by the tape. The films were allowed to air dry; then, they were sintered in the oven at 450°C for 30 minutes under oxygen flow. The films were cooled down before an immediate binding use, or were stored in a desiccator in the dark. Any difference was observed in a case of the films, which were stored for weeks as indicated.

The binding of C-153@ OA_2 complex onto $\text{TiO}_2/\text{ZrO}_2$ nanoparticle films was performed by immersing the suitable (MO_n) films in 1 mM aqueous solution of the hemicarceplex overnight in the dark. Then, the modified films were rinsed with D.I. water and dried in the oven at 110°C for 30 minutes before the spectroscopic measurements.

2.2 Results and Discussion.

From the published paper,²⁴ it is known that the C-153@ OA_2 complex (in aqueous borate buffer solution) at pH~9 was able to form a stable complex. However, during attachment of C-153@ OA_2 complex onto TiO_2 films (the modification of

semiconductor's film surface), it is shown that electron transfer from C-153 incarcerated inside OA to TiO_2 is dependent on the capsule stability and energy levels of TiO_2 . In general, any addition of acids or bases causes a significant shift of the TiO_2 conduction band edge (a Nernstian shift of $\sim 59 \text{ mV/pH}$).⁷ Usually, the injection from a photoreductant dye is favored in acidic condition (lowering of energy level of the conduction band, E_{cb}); however, strong basic conditions inhibit charge injection of the organic dye with an excited state close to the E_{cb} . Therefore, neutral or acidic conditions are more desirable; nevertheless, the solubility of OA is better at basic pH.⁷ Thereby, the pH influence on the complex stability was tested by recording the emission spectra of C-153@OA₂ (in aqueous solution) at different pH (Figure 2.7 a).

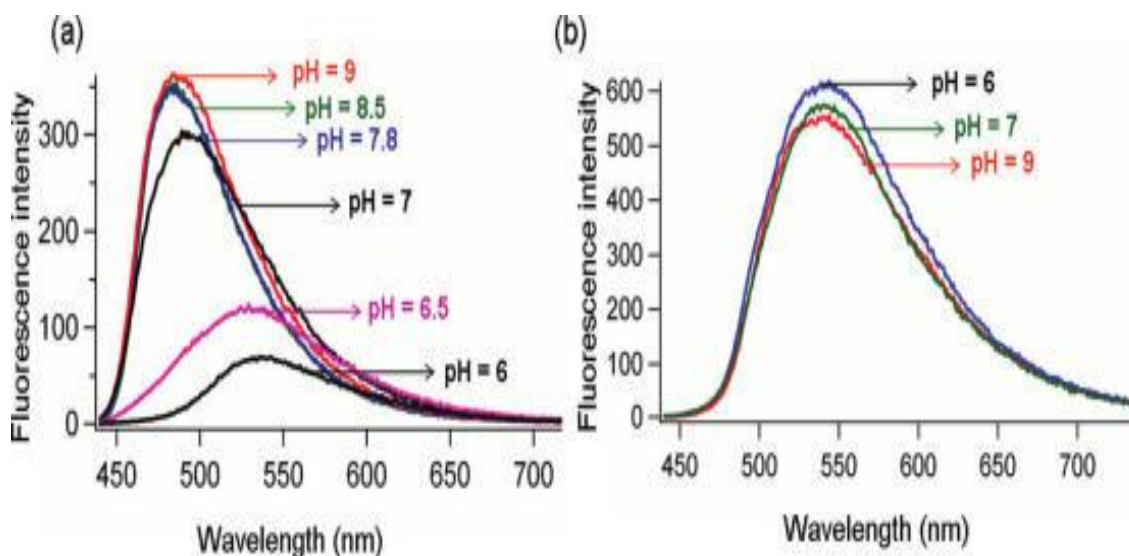


Figure 2.7 Fluorescence spectra of (a) C-153@OA₂ and (b) C-153 at different pH; $\lambda_{\text{ex}} = 420 \text{ nm}$; $[\text{C-153}] = 1.5 \times 10^{-5} \text{ M}$, $[\text{OA}] = 1 \times 10^{-4} \text{ M}$ in 10mM sodium tetraborate buffer(data from Porel M.).⁷

Then, dependent on the emission maximum of the complex, the C-153 location was determined relative to the capsule (encapsulated or free). Therefore, at pH9, the emission maximum of the complex was at 483 nm, what was considered as C-153 being inside the lipophilic capsule interior, but the shift to 535 nm at pH6 suggest dissociation of the complex under acidic conditions and a resulting decrease in water solubility (535 nm band intensity decreases). However, the emission maximum of the dye alone (C-153) did not show any dependence of the pH (Figure 2.7 b). Thus, based on all recorded emission spectra under different pH, we concluded that all experiments with modified TiO₂ should be carried out at pH7.⁷

The probing of the photoinduced electron-transfer from C-153@OA₂ complex to TiO₂ as a semiconductor included the use of two kinds of nanostructured TiO₂: thin films and a colloidal aqueous nanoparticle diluted solution. Nanostructured ZrO₂ was used as a control because it is considered an insulator (a wider band-gap than TiO₂, where ZrO₂ E_{bg} ~ 5.0 eV, but TiO₂ E_{bg} ~ 3.2 eV) and whose morphology closely resembles to TiO₂ films, and which electron injection from the photoexcited C-153@OA₂ complex is excluded (Figure 2.8 a). These comparisons can be easily seen in the emission spectra of modified ZrO₂ and TiO₂ films with C-153@OA₂ complexes (λ_{ex} = 420 nm), where the fluorescence emission of C-153@OA₂ was quenched in the case of TiO₂, but on ZrO₂ films was shown a broad fluorescence spectrum (corresponding to the emission in solution of C-153@OA₂). In addition, the encapsulated guest, which is shielded from a polar environment, can be bound to the metal oxide films without the necessity of its modification with an anchoring group, but C-153 in the absence of the host (OA) did not

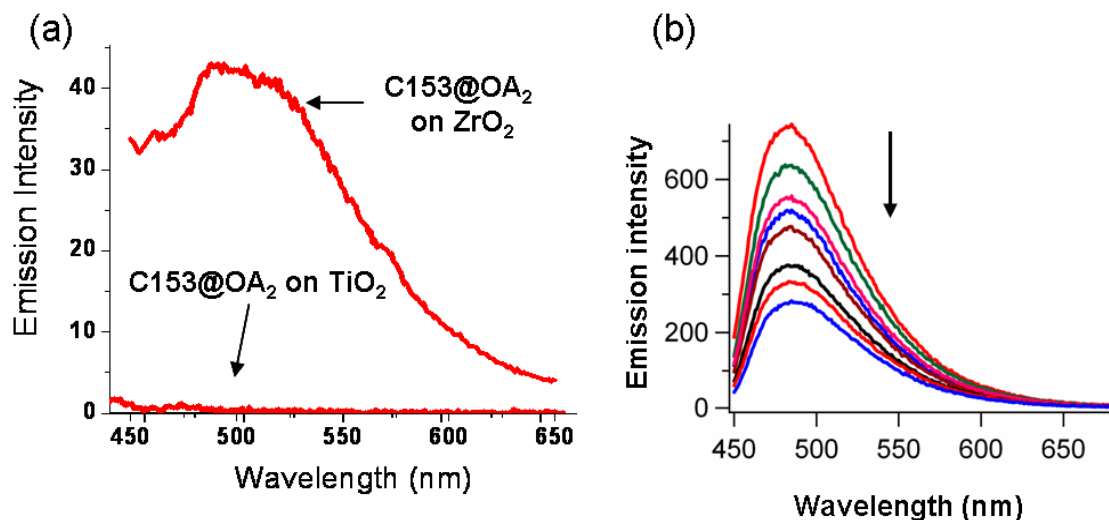


Figure 2.8 Fluorescence spectra of (a) C153@OA₂ on TiO₂ and ZrO₂ film, $\lambda_{\text{ex}} = 420$ nm; (b) titration of C153@OA₂ with TiO₂ solution; $\lambda_{\text{ex}} = 440$ nm; $[C153] = 1.5 \times 10^{-5}$ M, $[OA] = 1 \times 10^{-4}$ M in water.⁷

bind at all. Moreover, addition of the aqueous colloidal TiO₂ to the solution of C-153@OA₂ indicated that increasing the TiO₂ concentration decreased the complex's

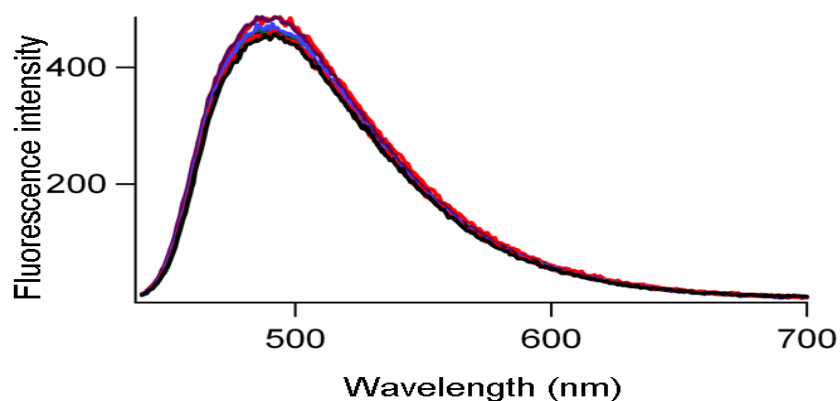


Figure 2.9 Fluorescence titration spectra of C153@OA₂ with ZrO₂ colloidal solution; $\lambda_{\text{ex}} = 440$ nm; $[C153] = 1.5 \times 10^{-5}$ M, $[OA] = 1 \times 10^{-4}$ M in water (data from Porel M.).⁷

fluorescence intensity, and behaved as a quencher. This effect is similar to that on a functionalized TiO_2 film (with C-153@OA_2), where the fluorescence was completely quenched. Nevertheless, there was no effect of colloidal ZrO_2 on the fluorescence emission intensity (Figure 2.9). Therefore, it can be concluded that the emission quenching in TiO_2 films must be the result of physisorption of C-153@OA_2 complex on the surface of TiO_2 .

The functionalized TiO_2 and ZrO_2 films (by immersing them inside 1mM aqueous solution of C-153@OA_2 at pH7) were monitored by FT-IR-ATR and compared with the OA (solid) spectrum (Figure 2.10). Thus, the band at $\sim 1708/1707 \text{ cm}^{-1}$, due to the $\nu(\text{C=O})$ stretch, indicates unbound COOH groups of OA, but the intense broad bands in the 1500-1650 region correlate to the $\nu(\text{O-C-O})$ stretch of bound carboxylate groups.

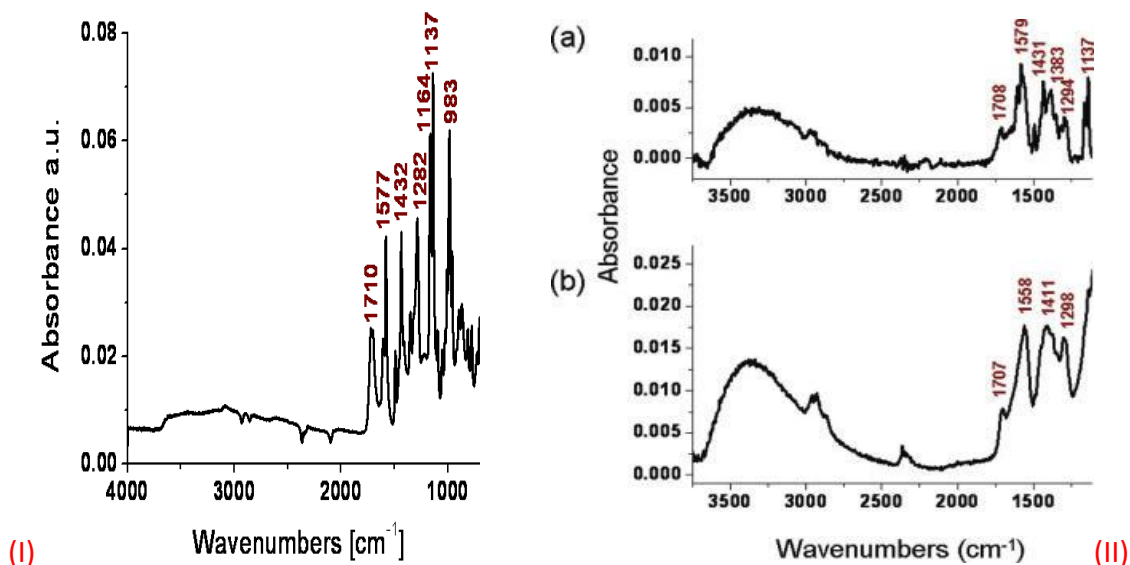


Figure 2.10 FT-IR-ATR spectra of OA (solid) (I); and of C-153@OA_2 on (a) TiO_2 and (b) ZrO_2 (II).⁷

Also, a band at $\sim 1294/1298\text{ cm}^{-1}$ due to the ν (C-O) stretch and a band above 3000 cm^{-1} due to the broad ν (O-H) stretch of COOH indicate that C-153@OA₂ complex was bound on both TiO₂ and ZrO₂ films (with comparison to the spectrum of OA as a powder).⁷

2.3. Conclusions.

The photoactive molecules, such as C-153, encapsulated within the macrocyclic host (C-153@OA₂) and attached onto semiconductor nanoparticle surfaces (TiO₂) cause new chemical or photophysical properties which can be useful for development of electronic devices, functional materials, DSSCs and others. The inclusion of the guest inside the host cavity and then binding to Metal Oxide films prevent negative effects, such as dye aggregation as well as dimerization processes and eliminate the need for synthetic modifications of the guest molecules with anchoring groups. In addition, C-153 without an encapsulation inside the OA lipophilic cavity was not able to bind to the surface of TiO₂ and ZrO₂ nanoparticle films because of the lack of binding groups. However, what was shown in this thesis, C-153 incarcerated within a host was able to be attached to TiO₂/ ZrO₂ films by anchoring groups of OA (multiple COOH groups), which more strongly interact with semiconductor surfaces than -OH and C=O. Also, the C-153@OA₂ complex bound to the TiO₂ film was able to transfer an electron from C-153 to TiO₂; however, the capsule stability was dependent on the pH. In neutral conditions, at pH7, the capsule of C-153@OA₂ was stable (not dissociated), and did bind to TiO₂/ ZrO₂ films; this was proved by the emission and FT-IR-ATR spectra of these modified films. Therefore, other photoinduced organic dyes can be used for encapsulation inside OA as a

macrocyclichost; however, the electron transfer process and its dynamics require additional studies.

References:

- (1) Peter L.M., The Gratzel Cell: Where Next? *J. Phys. Chem. Lett.* **2011**, 2, 1861-1867.
- (2) Hagfeldt A., Boschloo G., Sun L., Kloo L., Pettersson H.: Dye-Sensitized Solar Cells. *Chem. Rev.* **2010**, 110, 6595-6663.
- (3) Ardo S., Meyer G. J.: Photodriven Heterogeneous Charge Transfer with Transition-Metal Compounds Anchored to TiO₂ Semiconductor Surfaces. *Chem. Soc. Rev.* **2009**, 38, 115-164.
- (4) Paba C., Zordan G., Galoppini E., Piatnitski E. L., Hore S., Deshayes K., Piotrowiak P.: Hybrid Photoactive Assemblies: Electron Injection from Host-Guest Complexes into Semiconductor Nanoparticles. *J. Am. Chem. Soc.* **2004**, 126, 9888-9889.
- (5) Freitag M., Galoppini E.: Molecular Host-Guest Complexes: Shielding of Guests on Semiconductor Surfaces. *Energy Environ. Sci.* **2011**, 4, 2482-2494.
- (6) Ricci P.C., Pozzo A. Da., Palmas S., Muscas F., Carbonaro C.M.: Efficient Charge Transfer Process in Coumarin 153-Nanotubular TiO₂ Hybrid System. *Chem. Phys. Lett.* **2012**, 531, 160-163.
- (7) Porel M., Klimczak A., Freitag M., Galoppini E., Ramamurthy V.: Photoinduced Electron Transfer Across a Molecular Wall: Coumarin Dyes as Donors and Methylviologen and TiO₂ as Acceptors. *Langmuir* **2012**, 28, 3355-3359.
- (8) Zeng W., et al., *Chem Mater.* 2010, 22, 1915.
- (9) Chen C.-Y., Wang M., Li J.-Y., Pootrakulchote N., Allibabaei L., Ngoc-le C.H., Decoppet J.-D., Tsai J.-H., Gratzel C., Wu C.-G., Zakeeruddin S. M., Gratzel M.; *ACS Nano* **2009**, 3, 3103.
- (10) Yella A., et al., *Science* **2011**, 334, 629.
- (11) Hara K., Miyamoto K., Abe Y., Yanagida M.; *J. Phys. Chem. B Lett.* **2005**, 109, 23776.
- (12) Rehm J. M., McLendon G. L., Nagasawa Y., Yoshihara K., Moser J., Gratzel M.: *J. Phys. Chem.* **1996**, 100, 9577-9578.
- (13) Enea O., Moser J., Gratzel M.: *J. Electroanal. Chem.* **1989**, 259, 59.
- (14) Galoppini E., Thyagarajan S.: Organic Dyes Aggregation on TiO₂ Surfaces. *The Spectrum* **2005**, 18, (3), 22-27.
- (15) Serpone, N.; Pelizzetti, E. *Photocatalysis. Fundamentals and Applications*. John Wiley & Sons: New York, **1989**.
- (16) Kamat, P. V.; Meisel, D. *Semiconductor Nanoclusters: Physical, Chemical and Catalytic Aspects*. Elsevier: Amsterdam, **1997**.
- (17) Jortner, J.; Ratner, M. *Molecular Electronics*; Blackwell: London, **1997**.
- (18) Manera, M. G.; Leo, G.; Curri, M. L.; Cozzoli, P. D.; Rella, R.; Siciliano, P.; Agostiano, A.; Vasanelli, L. Investigation on Alcohol Vapours/TiO₂ Nanocrystal Thin Films Interaction by SPR Technique for Sensing Application. *Sensors and Actuators B* **2004**, 100, 75.
- (19) Comini, E.; Baratto, C.; Faglia, G.; Ferroni, M.; Sberveglieri, G. Single Crystal ZnO Nanowires as Optical and Conductometric Chemical Sensor. *J. Phys. D: Appl. Phys.* **2001**, 34, 569.

- (21) Martini, I.; Hodak, J. H.; Hartland, G. V. Effect of Structure on Electron Transfer Reactions Between Anthracene Dyes and TiO₂ Nanoparticles. *J. Phys. Chem. B* **1998**, 102, 9508.
- (22) Taratula, O.; Rochford, J.; Piotrowiak, P.; Galoppini, E.; Carlisle, R. A.; Meyer, G. J. Pyrene-Terminated Phenylethyne Rigid Linkers Anchored to Metal Oxide Nanoparticles. *J. Phys. Chem. B* **2006**, 110, 15734.
- (23) Wang Z.-S., Hara K., Danoh Y., Kasada C., Shionpo A., Suga S., Arakawa H., Sugihara H.: Photophysical and (Photo)-Electrochemical Properties of a Coumarin Dye. *J. Phys. Chem. B* **2005**, 109, 3907-3914.
- (24) Gupta S., Adhikari A., Mandal A. K., Bhattacharyya K., Ramamurthy V.: Ultrafast Singlet-Singlet Energy Transfer Between an Acceptor Electrostatically Attached to the Walls of an Organic Capsule and the Enclosed Donor. *J. Phys. Chem. C* **2011**, 115, 9593-9600.
- (25) Baldrige A., Samants S. R., Jayaraj N., Ramamurthy V., Tolbert L.M.; *J. Am. Chem. Soc.* **2010**, 132, 1498.
- (26) Porel M., Jayaraj N., Roghathama S., Ramamurthy V.; *Org. Lett.* **2010**, 12, 4544.
- (27) Jayaraj N., Zhao Y., Parthasarathy A., Porel M., Liu R. S. H., Ramamurthy V.: Molecules: Formation of Octa Acid Based Capsuleplex and Cavitandplex. *Langmuir* **2009**, 25, 10575-10586.
- (28) Gibb C. L. D., Gibb B. C.: Straight-Chain Alkanes Template the Assembly of Water-Soluble Nano-Capsules. *Chem. Commun.* **2007**, 16, 1635-1637.
- (29) Fraita M.: Host-Guest Chemistry Between Cucurbit[7]uril and Neutral and Cationic Guests. -thesis, **2011**.
- (30) Rochford, J.; Chu, D.; Hagfeldt, A.; Galoppini, E.: *J. Am. Chem. Soc.* **2007**, 129, 4655.

Chapter Three

Raman Spectroscopy as a Novel Promising Tool

for Analyzing a G-H Complex

of Ferrocene@CB[7]

Introduction

During the last decades the research of host-guest complexes between cucurbit[7]uril (CB[7]) and ferrocene (Fc) and its derivatives has received increasing interest.⁹⁻¹⁰ The solubilization of Fc (a hydrophobic guest) in an aqueous solution of CB[7] indicates formation of a complex with the neutral form of the guest (Fc@CB[7]); Kaifer and Kim have investigated the encapsulation of ferrocene inside CB[7] and published the X-ray crystal structure of the Fc@CB[7] complex (1:1) with two different orientations of the guest inside the host cavity interior.¹⁰ Moreover, all neutral and cationic ferrocenes and their derivatives form very stable complexes with CB[7], possessing binding constants in the 10^9 to 10^{13} M⁻¹ range.¹⁰ While there are numerous analytical methods to probe the formation and the structure of the Fc@CB[7] complexes, there are very few methods to study them in the solid state. Raman spectroscopy is a tool which can be successfully used for detection of the bonding and information about the structure of the host-guest complex formed in supramolecular chemistry. Also, Raman spectroscopy as a vibrational spectroscopic technique enables characterization of the supramolecular system and gives more advantages than infrared (IR) spectroscopy. Comparison of Raman spectroscopy with FT-IR proved that RS is more beneficial

Important note: Some of the sentences within this paragraph of this thesis were cited verbatim or slightly modified from the draft of paper on which we are working now and of which I am a co-author.

because of much better tolerance to water and CO_2 from atmosphere, so the acquired spectra are cleaner without harmonics and overtones.¹¹ Also, the possibility of acquisition of frequency vibrations which are below 600 cm^{-1} by RS is a big advantage compared to FT-IR.^{8,11} Moreover, it was previously reported^{12, 13} that probing the host-guest inclusion by FT-IR is not possible because of overlap of the IR bands of CB[7] with those deriving from encapsulated guests. However, Raman spectroscopy is more suitable for a detection of solid state H-G complexes because of its higher spectral resolution available for lower frequency modes (range).^{8, 11}

In this thesis, we present the use of Raman spectroscopy for studies of ferrocene encapsulation inside the CB[7] cavity in solid state (powder) form (Figure 3.1). An important part of this research was to show that Raman spectroscopy is a beneficial tool to confirm inclusion of the guest inside the host cavity interior in the solid state, and to investigate structural changes of a host and a guest during encapsulation.

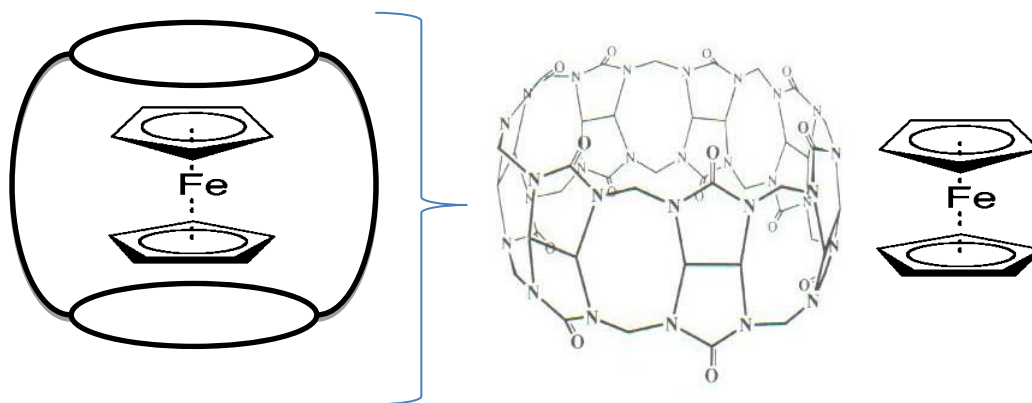


Figure 3.1 *The schematic illustration of the Fc@CB[7] 1:1 complex.*

Experimental Section

3.1 General.

^1H -NMR (499.896 MHz) spectra were collected on a Varian INOVA 500 NMR spectrometer at room temperature in D_2O . Chemical shifts acquired in ppm (δ) were reported relative to the central line of the solvent ($\delta_{\text{D}_2\text{O}}=4.82$ ppm). The chemicals used in this experiment were all analytical grade. Acetone, methanol (HPLC grade), ferrocene, glycoluril, formaldehyde (37% solution in water), α -cyano-4-hydroxy-cinnamic acid (CHCA) were used as received. Attenuated Total Reflectance Infrared (FT-IR-ATR) spectra were recorded at room temperature on a Thermo Scientific Nicolet 6700 Spectrometer, with 100 numbers of scan and a resolution of 4 cm^{-1} . High resolution mass spectra (MALDI-FTMS) were obtained on the departmental mass facility (BrukerDaltonics Apex-Qe series, Fourier Transform Mass Spectrometer) using CHCA as a matrix. The complex was mixed with a matrix solution ($\text{CH}_2\text{Cl}_2/\text{CHCl}_3$) in ratio of 1:2 (complex: matrix), and then after deposition on the plate, the mixture was allowed to dry by evaporation at room-temperature prior to the measurement. UV-Vis absorption spectra were acquired at ambient temperature on a Varian Cary-500 instrument using a Hewlett-Packard 8453 diode-array spectrometer. Spectrophotometric grade solvents were used for the spectroscopic and spectrometric measurements. The Raman spectra were collected in Prof. J. Lockard's group in our department using a Trivista triple monochromator and Spec-10 LN-cooled CCD detector (Princeton Instruments). A 785 nm laser at 26 mW was employed. Solid State CB[7], and ferrocene samples were prepared by grinding with ~ 80 wt% KNO_3 as internal standard and pressed pellets. Data were collected on spinning samples to minimize photodecomposition or thermal damage. The Fc@CB[7] complex was pressed with KNO_3 in a sample holder that did not allow

spinning due to the small sample amount. No evidence of photodecomposition or thermal damage was detected after multiple scans were collected.

3.1.1 Synthesis.

3.1.1.1 Cucurbit[7]uril.

CB7 was synthesized following mostly procedures published by Nau and coworkers,¹ and separation of the CB[n] homologues was adapted from the procedure described by Kim, and coworkers,²⁻³ however, some modifications were included (Figure 8). Formaldehyde (14 mL, 37% aqueous solution) was poured into a two-neck round bottom flask and after addition of sulfuric acid (60 mL, 9M aqueous solution), the solution was stirred (~ 15 min) in an ice-bath at 5°C in aerated conditions. Glycoluril (11.4g, 80 mmol) was added in one portion to the cold solution and then the reaction mixture was stirred (45 min) until it turned into a viscous, transparent solution. The flask was equipped with a condenser and the reaction mixture was heated at 90- 95°C for 72 h. The resulting orange viscous mixture was cooled to room temperature, and poured into 200 mL of D.I. water. Upon addition of acetone (800 mL,) a grey- white, semi-crystalline precipitate formed. The precipitate, which is a mixture of several CB[n] homologues, was separated by decantation, and the precipitate was washed with 1.5 L of a mixture of cold acetone/ water (8:2 v/v). Then, the grey-white precipitate was triturated with D.I. water (400 mL) to dissolve homologues other than CB6 by stirring for 30 min. and separated by filtration. The remaining solution was treated with acetone (300 mL) and a cloudy, white precipitate formed as a mixture of CB[7] and CB[5], which was left overnight before filtration. The previous filtrate solution of CB[n] homologues (after separation of CB6)

was evaporated to 1/3 volume and then treated with methanol (300 mL). The cloudy, white precipitate solution was left to settle for 1-3 days and then a white precipitate of CB[7] as a main product was separated by filtration (~95 % purity, without recrystallization, checked by ^1H -NMR (Figure 3.2). The precipitate of CB[5] and CB[7] was dissolved in 200 mL of D.I. water, and methanol (200 mL)

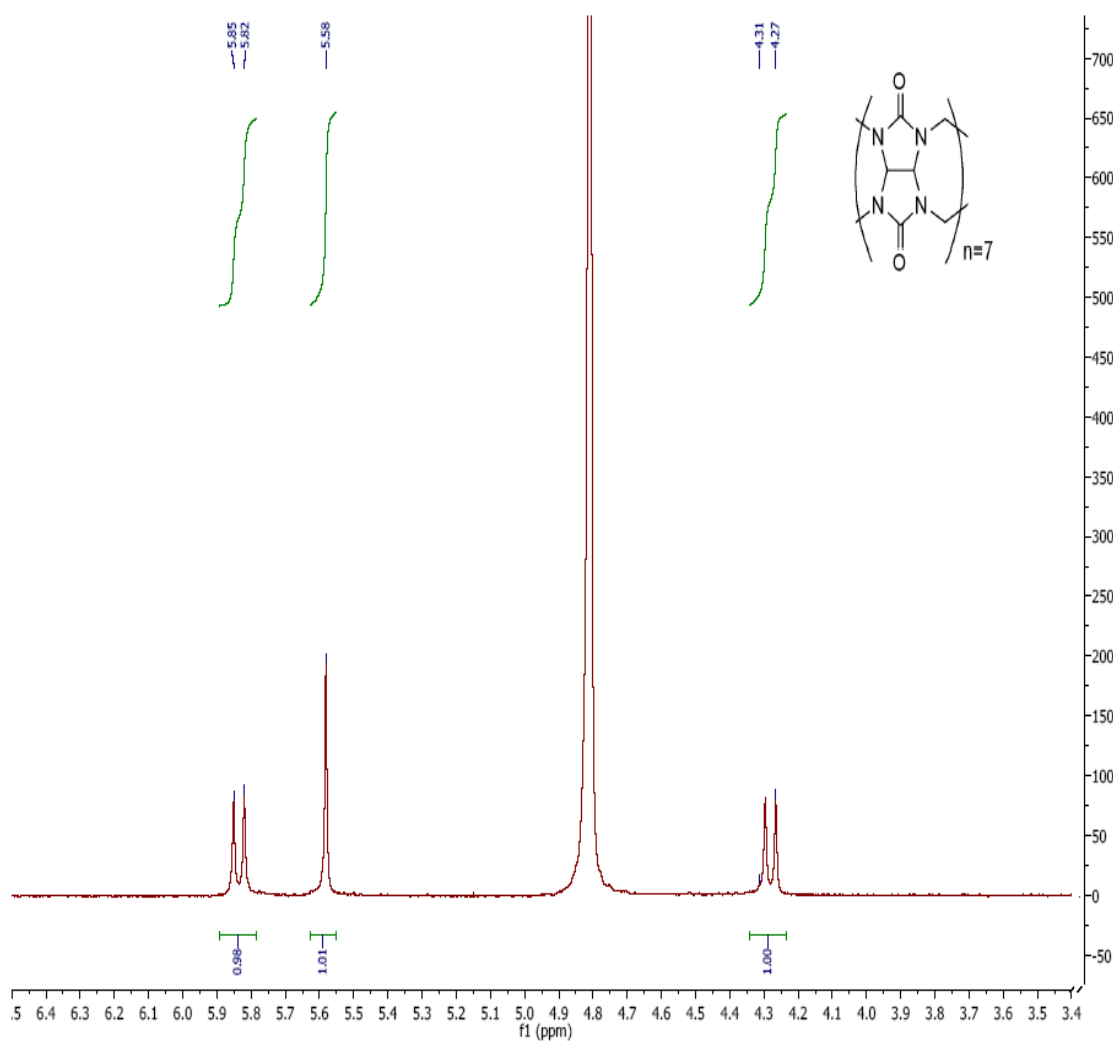


Figure 3.2 ^1H -NMR spectrum of CB[7] in D_2O (3.5-6.4 ppm region).

was added, resulting in the formation of a white precipitate of CB7 (Figure 3.3); however, it still contained traces of CB5. The product was dried under vacuum at 140 °C

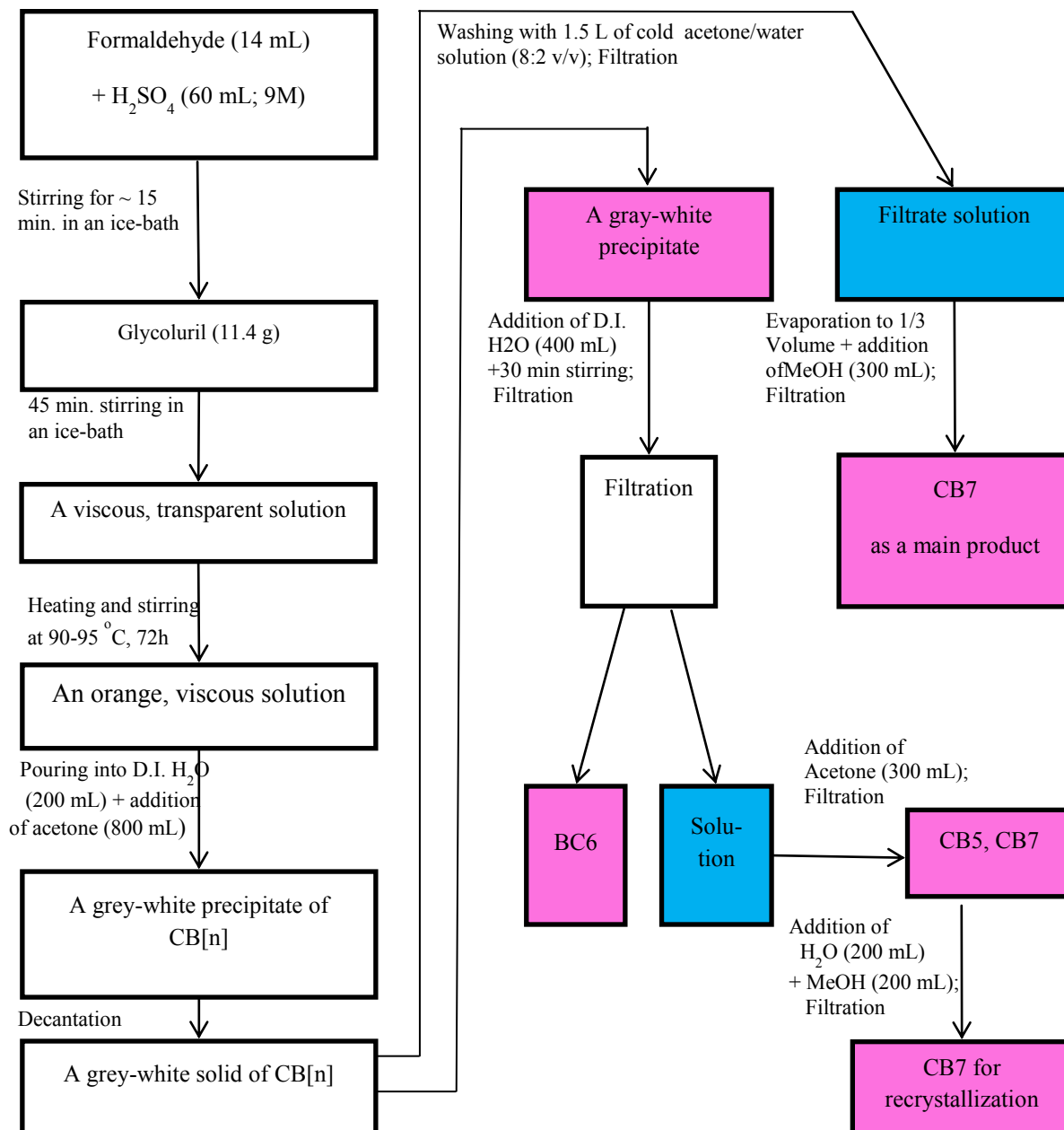


Figure 3.3 Synthesis and separation of CB7.

Boxes shaded in pink indicate precipitate, blue indicate solutions.

for 48 h. The spectral data were consistent with those reported in literature:^{2, 4-7} $^1\text{H-NMR}$ (D_2O): $\delta = 4.27\text{-}4.30$ ppm (d, $J = 15.5$, 14 H, CH_2), 5.58 ppm (s, 14 H, CH), 5.82-5.85 ppm (d, $J = 15.4$, 14 H, CH_2); FT-IR-ATR: ~ 3432 (N-H), 2925 (C-H), 1721 (C=O), 1634 (C=C), 1468 (C-N), 1373, 1320, 1219, 1185, 965, 800 cm^{-1} , MALDI m/z calcd for $[(\text{C}_6\text{H}_6\text{N}_4\text{O}_2)_7 + \text{Na}]^+$: 1185.3327; found: 1185.3334. calcd for $[(\text{C}_6\text{H}_6\text{N}_4\text{O}_2)_7 + \text{K}]^+$: 1201.3067; found: 1201.3066. Aqueous solutions of CB7 (as synthesized) are acidic and the pH was adjusted to pH 7 (by using aqueous HCl and NaOH) prior to the freeze-pump-thaw procedure described below, because we observed that ferrocenium formation was slower in neutral solution (See Figure 3.6).

3.1.2. Formation of Fc@CB[7] Complex.

The formation of the ferrocene@CB7 complex in de-aerated conditions was done in a quartz cuvette for freeze-pump-thaw equipped with a stirring-bar. The aqueous solution of CB7 (3 mL of a 1 mM solution, pH 7) was added to a quartz cuvette charged with ferrocene (0.6 mg, 0.003 mmol) and de-aerated by several freeze-pump-thaw cycles, followed by sonication. The resulting solution, maintained under vacuum in the sealed cuvette, was stirred overnight in the dark. UV-Vis spectra, collected immediately after formation of the complex and after one and a half weeks showed little change. The evaporation of the aqueous solution of the Fc@CB7 complex was done by quickly transferring under nitrogen the solution into a round bottom flask and by evaporating the water at high vacuum. The solid complex was then used for spectroscopic measurements.

3.2 Results and Discussion.

The UV-Vis spectrum of the ferrocene solution (a light-yellow color, 1mM in CH_3CN) showed an absorption peak at 440 nm, while Fc is insoluble in water. The aqueous solution of $\text{Fc@CB}[7]$ complex is oxidized by dissolved oxygen at an acidic pH; therefore, the pH of the complex solution was adjusted to 7 and the freeze-pump-thaw method was used to de-aerate the solution. UV-Vis spectra of the $\text{Fc@CB}[7]$ complex (light-yellow color, 1mM; pH7) in de-aerated conditions gave a blue shift at 402 nm after one and a half weeks. Therefore, from the spectra, we can conclude that the guest encapsulation inside the $\text{CB}[7]$ cavity is time dependent (the $\text{Fc@CB}[7]$ complex formed slowly) because $\text{CB}[7]$ is soluble in water at acidic pH, but not soluble at pH7. However,

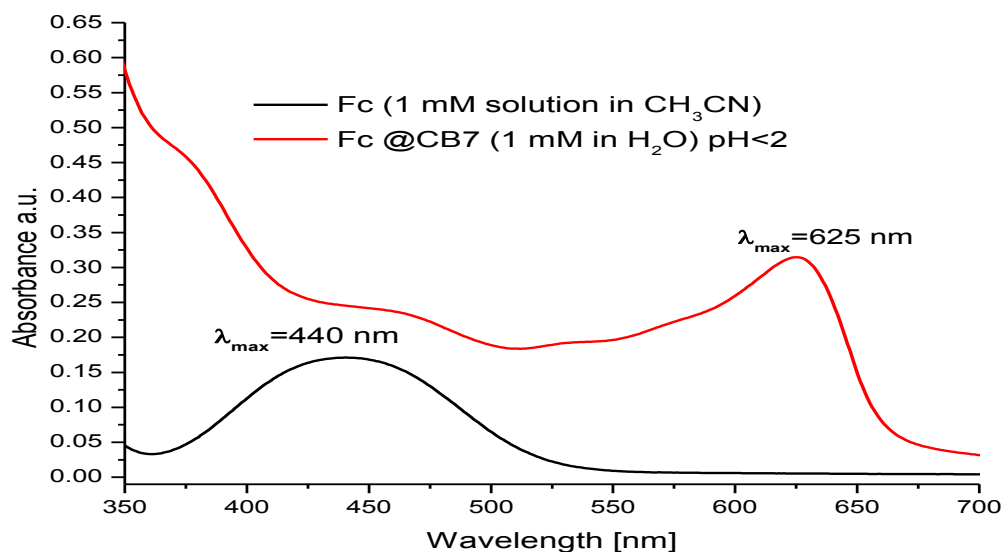


Figure 3.4 *Solution UV-Vis spectra of Fc and the $\text{Fc@CB}7$ complex in aerated conditions.*

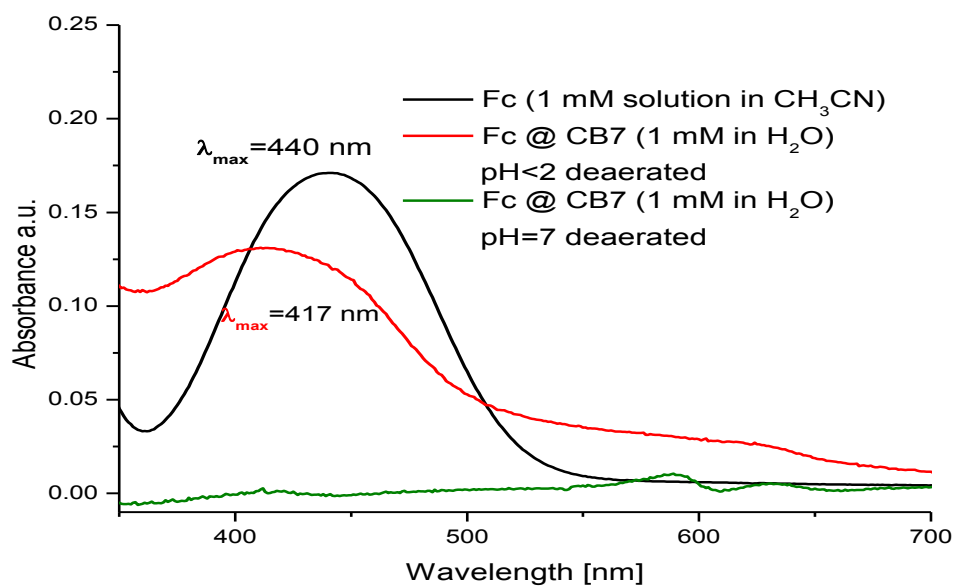


Figure 3.5 UV-Vis spectra of the Fc@CB7 complexes (pH<2 and pH=7) de-aerated by freeze-pump-thaw.

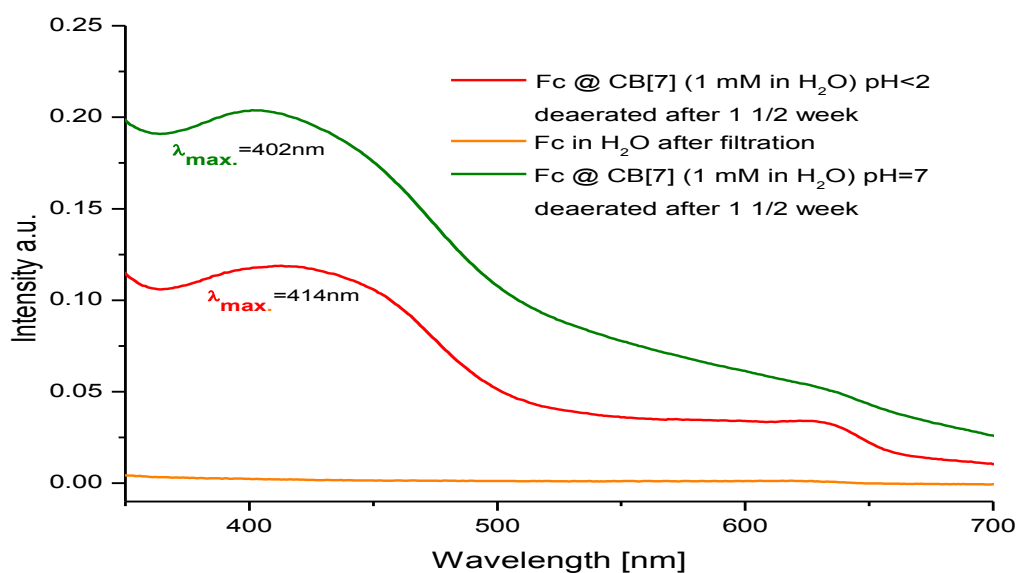


Figure 3.6 UV-Vis spectra of Fc@CB7 complexes (pH<2 and pH=7) after 1 1/2 weeks.

the Fc@CB[7] complex's oxidation to $\text{Fc}^+\text{@CB[7]}$ was slower at pH7. To attain the pH Fc@CB[7] complex, the solution was stored for several days. On the other hand, the Fc@CB[7] complex formed rapidly at $\text{pH} < 2$ in H_2O (in deaerated conditions), but overtime, there was some oxidation to the ferrocenium form of the complex ($\text{Fc}^+\text{@CB[7]}$), giving a pick at $\sim 625 \text{ nm}$ (Figure 3.6). The $\text{Fc}^+\text{@CB[7]}$ complex (a light-

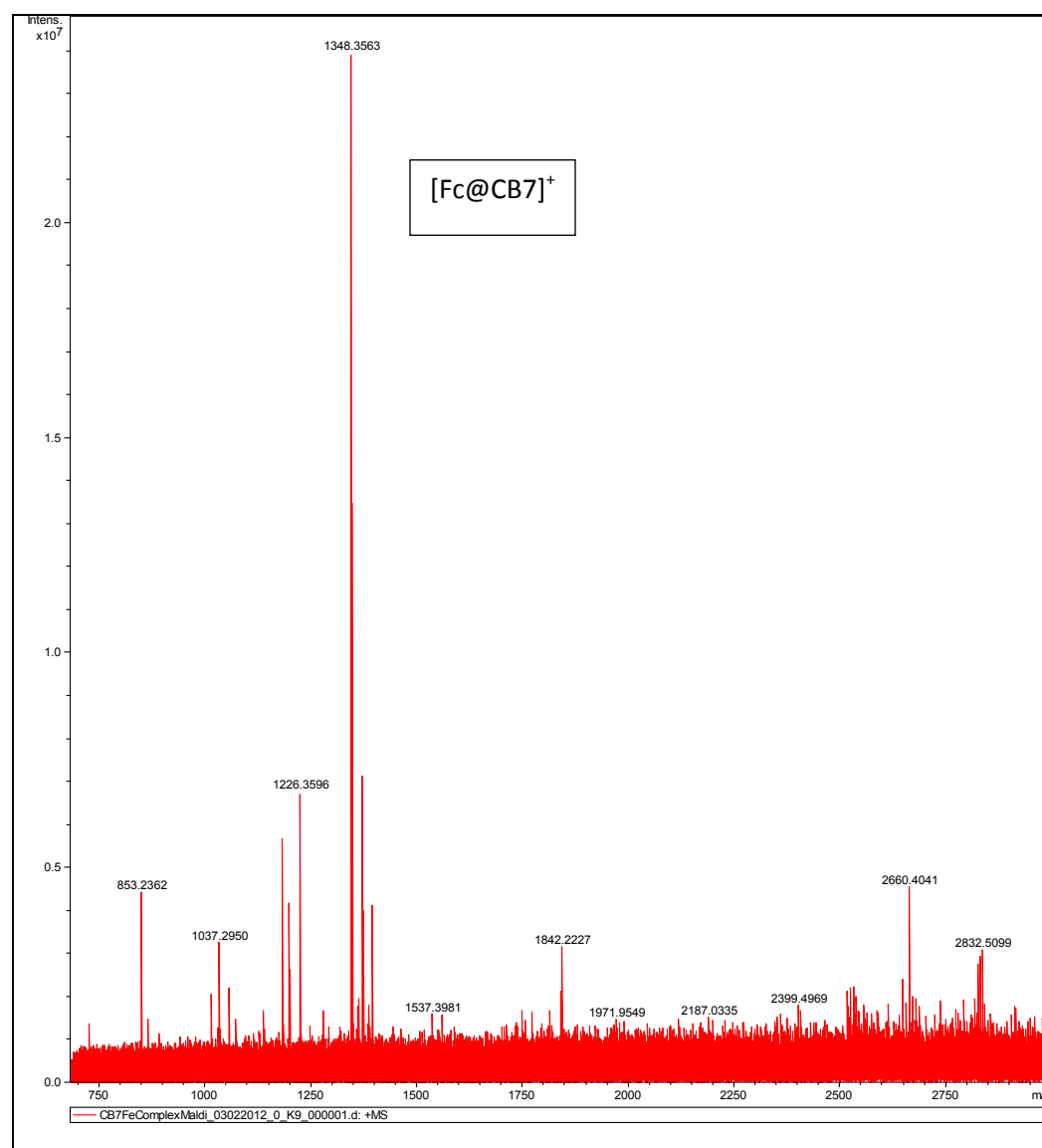


Figure 3.7 RMS-MALDI full window spectra of Fc@CB7 complex.

green color) is forming faster because of CB[7] tendency for encapsulation of positively-charged guests.

The MALDI-FTMS spectra showed the peaks for the Fc@CB[7] complex at m/z 1348.3563 (calcd. for [Fc@CB[7]]: 1348.3563), 1185.3334 (calcd. For [CB[7] +Na⁺]:

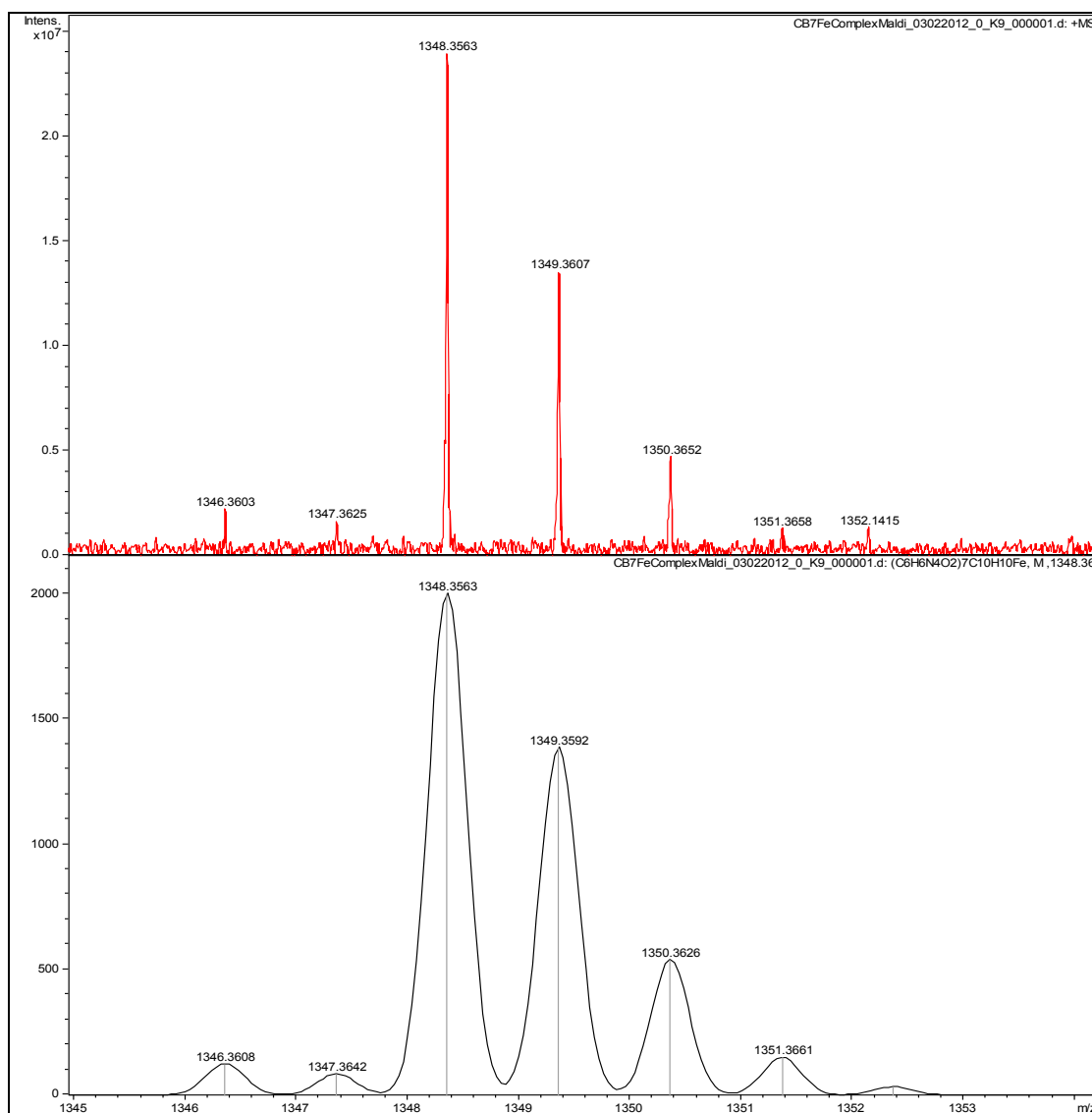


Figure 3.8 *HRMS-MALDI calculated isotopic pattern of the Fc@CB7 complex.*

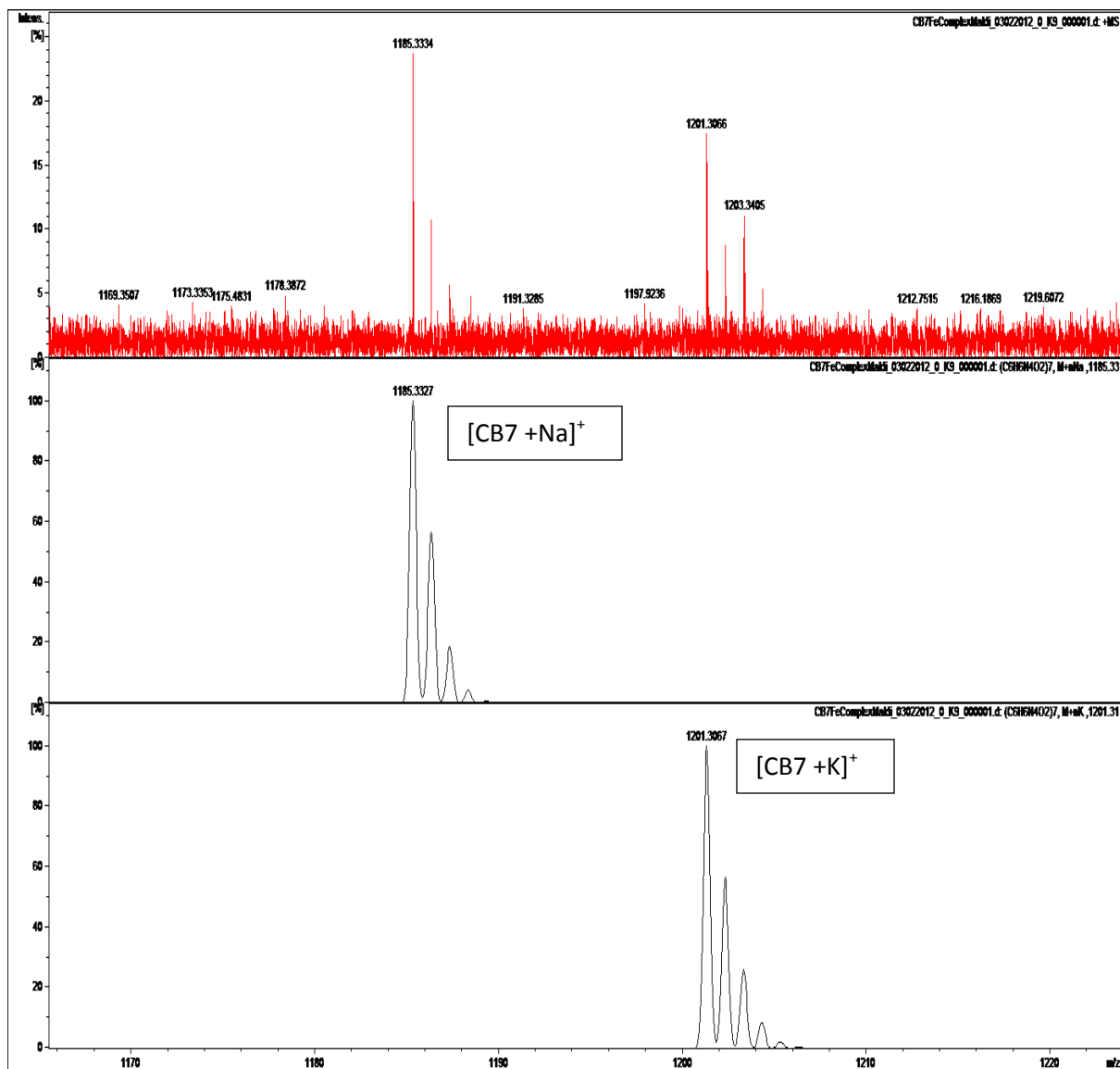


Figure 3.9 *HRMS-MALDI calculated isotopic pattern of CB7 from the Fc@CB7 complex spectra.*

1185.3327), and 1201.3066 (calcd. for $[CB[7] + K^+]$: 1201.3067)(see Figures 3.7-3.9), indicating that metal ions bind strongly to the complex, and that the complex is formed.

FT-IR-ATR was used to characterize the solid samples of Fc, CB[7] and Fc@CB[7] complex with KNO₃ (added as reference for Raman spectroscopy). The spectra showed C=C and C-H stretching bands of the cyclopentane rings at 3095, ~1700, 1409 cm⁻¹ and in the 800-1110 cm⁻¹ range. The encapsulation of the guest inside CB[7] by the FT-IR-

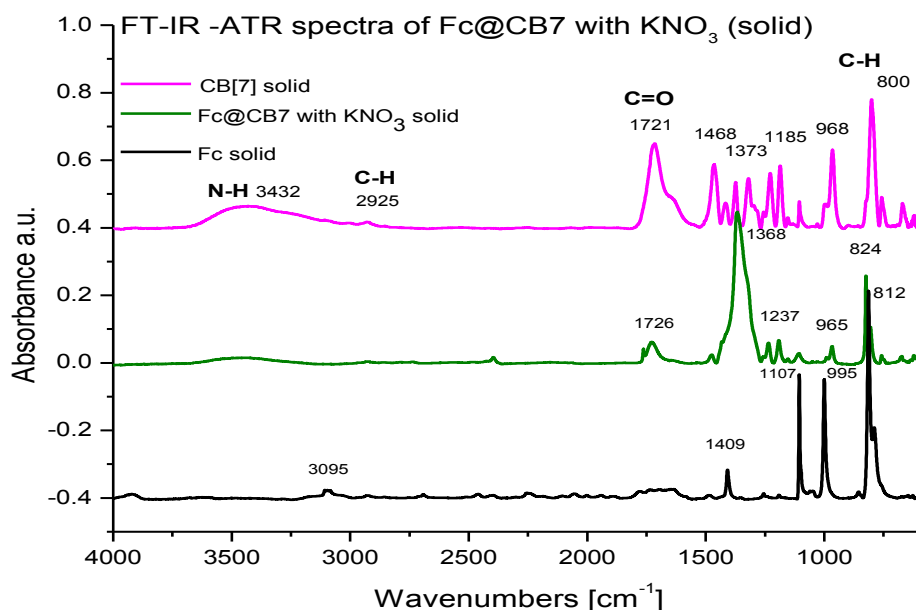


Figure 3.10 FT-IR-ATR spectra of solid CB7 (top), Fc (bottom) and Fc@CB7 with KNO₃(middle).

ATR spectra are difficult to probe because of considerable spectra overlap between the guest and the host. FT-IR spectra show that there is a need to use an alternative analytical technique to study these kinds of complexes in solid state environments. Therefore, Raman spectroscopy, which is a vibrational spectroscopy, is well-suited for this characterization. Also, higher spectral resolution and acquisition of lower frequency modes are the benefits of Raman which permit easily characterization of the Fc@CB[7]

complex because Raman bands attributed to both the CB[7] and Fc are able to be identified and resolved (Figure 3.11; all Raman frequency data are included in Table 3.1).

Figure 3.11(a) *Raman spectra of solid ferrocene (red), CB[7] (black) and Fc@CB[7] (blue) with KNO₃. Roman spectral ranges of (b) Fc and (c) CB[7] vibrational modes (NO₃ internal standard peaks indicated with *).*

In addition, the comparison of the vibrational frequency shifts (Fc, CB[7]) for various vibrational modes of the experimental Raman spectroscopy data, which were obtained by Prof. J. Lockard's group, gives us the evidence that the Fc guest molecule is inside the CB[7] cavity interior in the solid state. The data permit us to have some insights of structural and electronic interactions that happen during formation of the complex. Thus, there are two low frequency bands originating from Fc, first –the symmetric Fe-Cp ring stretch (307cm^{-1}) and second –ring tilt (391 cm^{-1}), which upon formation of a complex

Fc	Fc@CB7	Vibrational Assignment	Mode no.^b
307 cm^{-1}	318 cm^{-1}	$\nu\text{Fe-Cp}$	4
391	400	Cp ring tilt	16
997	994	$\beta\text{C-H} (\parallel)$	13
1059	-	$\beta\text{C-H} (\parallel)^c$	24
1104	1104	Cp ring breathing	3
1411	-	$\nu\text{C-C}^c$	15
CB7	Fc@CB7	Vibrational Assignment	
442	440	$\sigma\text{N-C-N}$	
654	655	$\tau\text{HC-CH}$	
834	829	$\delta\text{C-N-C} + \rho\text{CH}_2$	
899	900	$\beta\text{C-N-C} + \tau\text{ N-C-C-N} + \nu\text{C-C}$	
1382	-	Sym. $\nu\text{C-N}^c$	
1425	1426	Asym. $\nu\text{C-N}$	
1760	1755	$\nu\text{C=O}$	

\parallel is with respect to the Cp ring plane. a. vibrational mode assignments for Fc and CB7 obtained from reference [17] and [16] respectively b. from normal mode notation used in reference [17] c. overlap with other Raman peaks prevents accurate frequency determination.

Table 2.1 *Comparison of Raman frequencies of Fc, CB7 and Fc@CB7 and corresponding vibrational mode assignments^a*

with CB[7] influence increase in frequency (318, 400 cm^{-1}). These vibrational frequency shifts that indicate higher force constants of these modes can be due to restricted motion along these vibrational coordinates for the Fc molecule constrained inside the CB[7] interior (similar behavior in force constant changes of Fc derivatives have been reported before ¹⁴).

The encapsulation of Fc within the CB[7] macrocycle also influences small changes of the vibrational modes of CB[7], and exhibits two distortion modes (442, 833 cm^{-1}). The inclusion of the guest molecule inside the host interior influences some deformation of the host cavity, which can show up at lower frequencies. Moreover, the reduced force constants for both of these modes are the effect of weak interactions between the C and N atoms of the host cavity and peripheral hydrogens of the Cp rings of Fc that may be due to expansion of the CB[7] host during encapsulation of the guest.¹⁰ However, as expected, there is only little or no effect on the force constants of the modes dominated by atomic displacements of the CB[7] exterior upon Fc encapsulation (such as the 654 cm^{-1} CB HC-CH twist mode). Also, the ring deformation mode (899 cm^{-1}) and both symmetric and asymmetric CB[7] C-N stretching modes (1382 and 1425 cm^{-1}) show a similar tendency.

Some of these described vibrational frequency changes can be explained by steric interactions that, during formation of the complex, may restrain certain vibrational motions. For instance, the electronic interactions between carbonyl groups of CB[7] (electron-donating) and Fc may affect some shift of the vibrational mode frequencies,

such as constraining the Cp ring breathing mode upon encapsulation that might increase its force constant; nevertheless, the opposite effect has been reported before.¹⁵

The increased force constants may appear because of electrostatic effects on CH bending modes of the Cp ring that increase positive charge on the Cp ring.¹⁸ Therefore, the observed downshift (lower frequency constant) mode of the Cp C-H bending (from 998 to 994 cm^{-1}) may appear because of interaction of Fc with C=O groups in the complex, which decreases the positive charge on the ring.

The previous study of the $\text{Fc@CB}[7]$ complex crystal structure,¹⁰ reported two different orientations of the Fc molecule within the solid-state complex. Therefore, our Raman spectra rather are representing an average of the Fc-guest orientation. Moreover, another factor that can influence the vibrational modes of the $\text{Fc@CB}[7]$ complex is the effect of counterions (such as cations in solution) which coordinate with the complex; nevertheless, in the solid-state form of the complex, it is not clear what happens with these cations.

3.3 Conclusions.

In summary, UV-Vis spectra of the $\text{Fc@CB}[7]$ complex solutions indicate oxidation of the encapsulated guest by dissolved oxygen. Therefore, the $\text{Fc@CB}[7]$ complex was de-aerated by freeze-pump-thaw and probed at two different pH ($\text{pH} < 2$ and $\text{pH} = 7$), indicating that the formation of the complex in H_2O is rapid at acidic pH (< 2), but over time, there is some oxidation to the ferrocenium form of the complex ($\text{Fc}^+\text{@CB}[7]$). Nevertheless, the $\text{Fc@CB}[7]$ complex at pH 7 in H_2O forms slowly, but the oxidation of the complex is minimized. This experiment was performed once and the influence of pH

on oxidation will require further investigation. The formation of the complex was time dependent, giving a blue shift (from 440 to 402 nm) after one and a half weeks. Also, MALDI-FTMS spectra confirm the formation of the Fc@CB[7] (1:1) complex by exhibiting a high intensity peak at m/z 1348.3563 (calcd. for [Fc@CB[7]]: 1348.3563). Nevertheless, FT-IR spectra of solid samples of Fc, CB[7] and the Fc@CB[7] complex were difficult to distinguish because of their overlapping peaks. Therefore, Raman spectroscopy was used to study structural changes that happen upon formation of the Fc@CB7 complex. Raman spectra, in collaboration with Prof. J. Lockard's group, show that specific vibrational modes localized on different parts of the complex were easily observed giving the proof that Fc is encapsulated within the CB[7] cavity, and exhibiting some structural and electronic interactions between the host and the guest components.

REFERENCES:

- (1) Marquez, C.; Huang, F.; Nau, W. M.: Cucurbiturils: Molecular Nanocapsules for Time-Resolved Fluorescence-Based Assays. *IEEE T. NANOBIOSCI.*, **2004**, 3, 39-45.
- (2) Kim, J.; Jung, I.-S.; Kim, S.-Y.; Lee, E.; Kang, J.-K.; Sakamoto, S.; Yamaguchi, K.; Kim, K.: New Cucurbituril Homologues: Syntheses, Isolation, Characterization, and X-ray Crystal Structures of Cucurbit[n]uril (n = 5, 7, and 8). *J. Am. Chem. Soc.* **2000**, 122, 540-541.
- (3) Zhao, J.; Kim, H.-J.; Oh, J.; Kim, S.-Y.; Lee, J. W.; Sakamoto, S.; Yamaguchi, K.; Kim, K.: Cucurbit[n]uril Derivatives Soluble in Water and Organic Solvents. *Angew. Chem. Int. Ed.* **2001**, 113, 4363-4365.
- (4) Silva J. P.; Jayaraj N.; Jockusch S.; Turro N.; Ramamurthy V. : Aggregates of Cucurbituril Complexes in the Gas Phase. *Org. Lett.* **2011**, 13 (9), 2410-2413.
- (5) Pischel U.; Uzunova V. D.; Remon P.; Nau W. R.: Supramolecular Logic with Macrocyclic Input and Competitive Reset. *Chem. Commun.* **2010**, 46, 2635-2637.
- (6) Carvalho C. P.; Uzunova V. D.; Silva J. P.; Nau W.M.; Pischel U.: A Photoinduced pH Jump Applied to Drug Release from Cucurbit[7]uril. *Chem. Commun.* **2011**, 47, 8793-8795.
- (7) Freitag M.; Galoppini E.: Cucurbituril Complexes of Viologens Bound to TiO₂ Films. *Langmuir* **2010**, 26 (11), 8262-8269.
- (8) Witlicki E. H., Hansen S. W., Christensen M., Hansen T. S., Nygaard S. D., Jeppesen J. O., Wong E. W., Jensen L., Flood A. H.: Determination of Binding Strengths of a Host-Guest Complex Using Resonance Raman Scattering. *J. Phys. Chem. A* **2009**, 113, 9450-9457.
- (9) Ong W.; Kaifer A. E.: Unusual: Electrochemical Properties of the Inclusion Complexes of Ferrocenium and Cobaltocenium with Cucurbit[7]uril. *Organometallics* **2003**, 22, 4181-4183.
- (10) Jeon W. S.; Moon K.; Park S. H.; Chun H.; Ko Y. H.; Lee J. Y.; Lee E. S.; Samal S.; Selvapalam N.; Rekharsky M. V.; Sindelar V.; Sobransingh D.; Inoue Y.; Kaifer A.E.; Kim K.: Complexation of Ferrocene Derivatives by the Cucurbit[7]uril Host: A Comparative Study of the Cucurbituril and Cyclodextrin Host Families. *J. Am. Chem. Soc.* **2005**, 127, 12984-12989.
- (11) Mahajan S.; Lee T.-C.; Biedermann F.; Hugall J. T.; Baumberg J. J.; Scherman O. A.; Roman and SERS Spectroscopy of Cucurbit[n]urils. *Phys. Chem. Chem. Phys.* **2010**, 12, 10429-10433.
- (12) Freitag M.: Host-Guest Chemistry Between Cucurbit[7]uril and Neutral and Cationic Guests.-thesis, **2011**.
- (13) Kazachkin, D. V.; Nishimura, Y.; Witek, H. A.; Irle, S.; Borguet, E.: Dramatic Reduction of IR Vibrational Cross Sections of Molecules Encapsulated in Carbon Nanotubes. *J. Am. Chem. Soc.* **2011**, 133, 8191-8198.
- (14) Butler, I. S.; Harvey, P. D.; Allen, G. C.: *J. Ram. Spec.* **1987**, 18, 1.
- (15) Dutta, P. K.; Thompson, M.: *J. Chem. Phys. Lett.* **1986**, 131, 435.

- (16) Heise, H. M.; Kuckuk, R.; Bereck, A.; Riegel, D., Infrared Spectroscopy and Raman Spectroscopy of Cyclodextrin Derivatives and Their Ferrocene Inclusion Complexes. *Vib. Spectrosc.***2010**,*53* (1), 19-23.
- (17) Bodenheimer, J. S.; Low, W., A Vibrational Study of Ferrocene and Ruthenocene. *Spectrochim. Acta A* **1973**,*29* (9), 1733-1743.
- (18) Diana, E.; Rossetti, R.; Stanghellini, P. L.; Kettle, S. F. A., Vibrational Study of (η^5 -Cyclopentadienyl)metal Complexes. *Inorg. Chem.***1997**,*36* (3), 382-391.

Curriculum Vitae
Agnieszka M. Klimczak

56 Neptune Pl.
Colonia, NJ 07067

Email: aklimczak15@gmail.com

EDUCATION AND PROFESSIONAL EXPERIENCE

08/2009-07/2012 Chemistry Department, **Rutgers University**, Newark, NJ

Expected Graduation M.S. Candidate (07.27.12)

Dissertation: Host-Guest complexes, their characterization by spectroscopic tools and photoinduced electron transfer on Metal Oxide surfaces.

Adviser: Prof. Elena Galoppini

09/2006-05/2009 ESL Program, **Union County College**, Elizabeth, NJ

01/1999-02/1999 Practical Training, Chemistry Department, **Rzeszow University of Technology**, Poland

09/1994-06/1999 Chemistry Department, **Rzeszow University of Technology**, Poland

Masters of Science Degree in Chemistry

Dissertation: Dissolution of some nitrogen containing bases in reactive solvents – new adhesive materials- polymers.

Adviser: Prof. Renata Lubczak

07/1997-08/1997 **POLMOS Distillery**, Lancut, Poland

Summer 2011 Teaching Assistant, ACS Proj. SEED Program, **Rutgers University**, Newark, NJ

Assisted a student from North Bergen H.S. in conducting research in an academic laboratory.

RESEARCH EXPERIENCE

Host-Guest Chemistry (Supramolecular Chemistry)

Organic synthesis (TiO₂, ZrO₂ nanoparticles, Cucurbit[7]uril and others)

Conducted binding study of Host-Guest complexes on the TiO₂ and ZrO₂

nanoparticle surfaces, prepared the surface of TiO₂ and ZrO₂ semiconductors films

(surface functionalization), and checked photophysical and photochemical properties of H-G complexes via instrumental analysis (FT-IR, UV-Vis, NMR, MALDI-FTMS, RS)

PUBLICATION

1) ***PHOTOINDUCED ELECTRON TRANSFER ACROSS a MOLECULAR WALL: COUMARIN DYES as DONORS and METHYL VIOLOGEN and TiO₂ as ACCEPTORS***

M. Porel, A. Klimczak, M. Freitag, E. Galoppini, V. Ramamurthy, *Langmuir* **2012** 28(7), 3355-3359.

2) ***STRUCTURAL INTERROGATION of a CUCURBIT[7]URIL-FERROCENE HOST-GUEST COMPLEX in the SOLID STATE: a RAMAN SPECTROSCOPY STUDY***

Y. Chen, A. Klimczak, E. Galoppini, J. V. Lockard, *submitted*

TEACHING and WORK EXPERIENCE

09/2011-05/2012 Teaching Assistant, World of Chemistry Laboratory (General and Organic Chemistry), Rutgers University, Newark, NJ

08/2009-07/2011 Teaching Assistant, General Chemistry Laboratory, Rutgers University, Newark, NJ